Geophysical Journal International

Geophys. J. Int. (2010) **183,** 572–586 doi: 10.1111/j.1365-246X.2010.04779.x

Structure across the northeastern margin of Flemish Cap, offshore Newfoundland from Erable multichannel seismic reflection profiles: evidence for a transtensional rifting environment

J. Kim Welford,[1] Jeremy Hall,[1] Jean-Claude Sibuet[2] and Shiri P. Srivastava[3]

[1] *Department of Earth Sciences, Memorial University of Newfoundland, St. John's, NL, Canada. E-mail: kwelford@mun.ca*
[2] *Ifremer, Centre de Brest, Département des Géosciences Marines, Plouzané, France*
[3] *Geological Survey of Canada (GSC), Bedford Institute of Oceanography, Dartmouth, NS, Canada*

Accepted 2010 August 17. Received 2010 August 7; in original form 2010 April 6

SUMMARY

We present the results from processing and interpreting nine multichannel seismic reflection lines collected during the 1992 Erable experiment over the northeastern margin of Flemish Cap offshore Newfoundland. These lines, combined into five cross-sections, provide increased seismic coverage over this lightly probed section of the margin and reveal tectonically significant along-strike variations in the degree and compartmentalization of crustal thinning. Similar to the southeastern margins of Flemish Cap and the Grand Banks, a transitional zone of exhumed serpentinized mantle is interpreted between thinned continental and oceanic crust. The 25 km wide transitional zone bears similarities to the 120 km wide transitional zone interpreted as exhumed serpentinized mantle on the conjugate Irish Atlantic margin but the significant width difference is suggestive of an asymmetric conjugate pair. A 40–50 km wide zone of inferred strike-slip shearing is interpreted and observed to extend along most of the northeastern margin of Flemish Cap. Individual shear zones (SZs) may represent extensions of SZs and normal faults within the Orphan Basin providing further evidence for the rotation and displacement of Flemish Cap out of Orphan Basin. The asymmetry between the Flemish Cap and Irish conjugate pairs is likely due in large part to the rotation and displacement of Flemish Cap which resulted in the Flemish Cap margin displaying features of both a strike-slip margin and an extensional margin.

Key words: Controlled source seismology; Continental margins: divergent; Continental tectonics: extensional; Submarine tectonics and volcanism; Crustal structure; Atlantic Ocean.

1 INTRODUCTION

While the Newfoundland/Iberia and Flemish Cap/Galicia Bank conjugate continental margins are arguably the best studied examples of non-volcanic/magma-poor margins in the world, relatively little attention has been focused on the neighbouring Flemish Cap–Orphan Basin/Goban Spur–Irish conjugate continental margins (Fig. 1). These margins are also non-volcanic/magma-poor and so offer an equally good location for studying the dynamics of rifting since magmatic processes have not altered or obscured their extensional crustal structures. As to the south, the nature of the transitional zone between continental and oceanic crust represents one key focus of investigation for all non-volcanic/magma-poor margins (Louden & Chian 1999; Srivastava *et al.* 2000; Whitmarsh *et al.* 2001a; Russell & Whitmarsh 2003) and in particular for the Flemish Cap margin and its conjugate. Outboard of Goban Spur on the Irish margin, seismic refraction modelling results have revealed exhumed serpentinized mantle between continental and oceanic crust (Bullock & Minshull 2005), similar to what has been observed off the Newfoundland, Iberia and Galicia Bank margins (Boillot *et al.* 1987; Pickup *et al.* 1996; Whitmarsh *et al.* 1996; Dean *et al.* 2000; Whitmarsh & Wallace 2001; Lau *et al.* 2006a,b; Shillington *et al.* 2006; van Avendonk *et al.* 2006; Deemer *et al.* 2009; Welford *et al.* 2010a). Meanwhile, preliminary results from recent seismic refraction surveying off the northeastern margin of Flemish Cap do show evidence for mantle exhumation but over a more limited spatial extent (Gerlings *et al.* 2009). With the increased seismic coverage provided by the Erable lines over the northeastern Flemish Cap margin, a better characterization of the transition zone's distribution along the entire margin is now possible. Furthermore, this seismic coverage provides a means for searching for structures associated with the hypothesized rotation and southward migration of Flemish Cap from out of Orphan Basin (Enachescu *et al.* 2005; Sibuet *et al.* 2007b).

The 1992 Erable project was undertaken jointly by the GSC's Atlantic Geoscience Centre (AGC) and the Institut français de

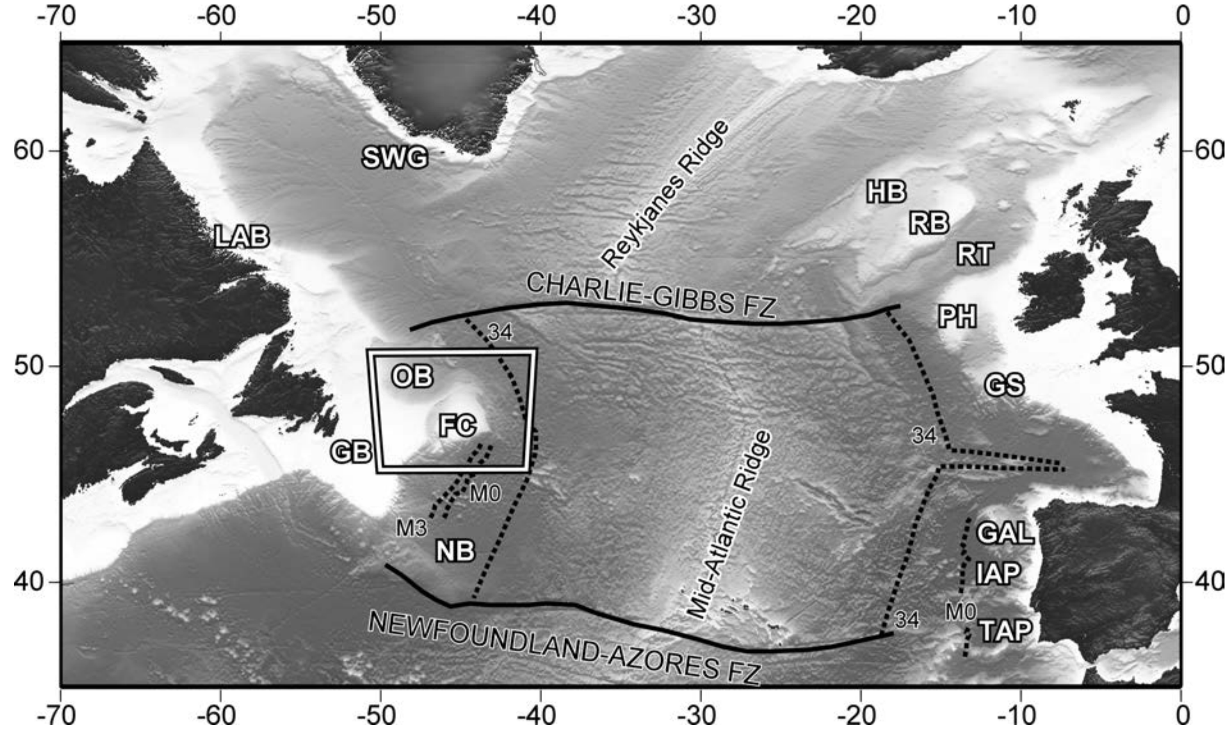

Figure 1. Bathymetric map of the North Atlantic region, adapted from Chian *et al.* (1999). Locations of magnetic anomalies 34, M0 and M3 (from Srivastava *et al.* 1988b, 1990, 2000) are plotted as dotted line segments. Outlined white box corresponds to our study area offshore Newfoundland. Abbreviations: GB, Grand Banks; OB, Orphan Basin; FC, Flemish Cap; NB, Newfoundland Basin; HB, Hatton Bank; RB, Rockall Bank; RT, Rockall Trough; PH, Porcupine High; GS, Goban Spur; GAL, Galicia Bank; IAP, Iberia Abyssal Plain; TAP, Tagus Abyssal Plain; LAB, Labrador margin; SWG, Southwest Greenland margin; FZ, fracture zone.

recherche pour l'exploitation de la mer (Ifremer). The project involved the acquisition of multiple 2-D multichannel seismic reflection profiles in the Newfoundland Basin and across the margins of Flemish Cap. We present and provide interpretations for nine of the profiles which extend across the northeastern margin of Flemish Cap, namely profiles E43, E44, E46, E47, E48, E49, E50, E51 and E52 (Fig. 2). We combine the results from the Erable profiles with those from multichannel seismic reflection profiles F85-3, F87-3 and F87-4 from the Frontier Geoscience Project (de Voogd & Keen 1987; Keen & de Voogd 1988; Reid & Keen 1990) to investigate the transition from continental to oceanic crust and to track variations in rifting style along the entire northeastern margin of Flemish Cap. These results are then compared with available constraints from the conjugate Irish Atlantic continental margin to enable discussion of the timing of rifting, rifting processes and the influence (if it occurred) of the clockwise rotation and southward migration of Flemish Cap.

2 TECTONIC SETTING OF THE FLEMISH CAP AND ORPHAN BASIN MARGINS

The continental shelf of the offshore Newfoundland margin consists of the Grand Banks and Flemish Cap which themselves consist of basement rocks of the Avalon terrane. During the Appalachian Orogeny in Paleozoic time, the Gondwanan Avalon terrane was accreted to the eastern margin of North America (Laurentia) during the closing of the Iapetus ocean (Haworth & Keen 1979; Williams 1984, 1995). Mesozoic opening of the modern North Atlantic ocean later occurred within this terrane. From paleoreconstructions of the margin in Cenomanian time (magnetic chron 34) at the inferred initiation of seafloor spreading (e.g. Srivastava *et al.* 1988b), the conjugates for the northeastern margins of Flemish Cap and Orphan Basin were the Goban Spur and the Porcupine High, offshore Ireland, respectively.

To the northeast of the Grand Banks, Flemish Cap, the focus of this study, is a prominent subcircular submarine knoll cored by Hadrynian (Late Proterozoic) rocks of the Avalon terrane (King *et al.* 1985; Enachescu 1992). This 30 km thick block of continental crust lies under less than 200 m of water and is flat-topped with a thin cover of Mesozoic–Cenozoic sediments that are folded and faulted along the west and southwest edge of the cap. With a hypothesized tectonic history involving significant clockwise rotation and southward migration over 200 km out of Orphan Basin (Srivastava & Verhoef 1992; Enachescu 2006; Sibuet *et al.* 2007b) —an enormous deep water basin to the north of the Grand Banks and to the northwest of Flemish Cap—the Flemish Cap represents a unique research target at the centre of the complex rifting environment of the North Atlantic.

Separation of Iberia and Eurasia from North America was preceded by an initial rifting episode during the Triassic which created many of the half graben found on the Grand Banks (e.g. Carson-Bonnition, Jeanne d'Arc, Whale, Horseshoe), in the East Orphan Basin (Enachescu *et al.* 2004c; Enachescu 2006), on the Irish margin (e.g. Celtic Sea, Porcupine, Western Approaches; Naylor & Shannon 2009) and on the Galicia Bank margin (e.g. Inner Galicia, Lusitanian; Murillas *et al.* 1990) while the Flemish Cap was not affected until the early Jurassic (Sibuet *et al.* 2007b). A second phase of rifting from the Late Jurassic to the Early Cretaceous which progressed diachronously from south to north led to the east-west separation of the Grand Banks from central Iberia and

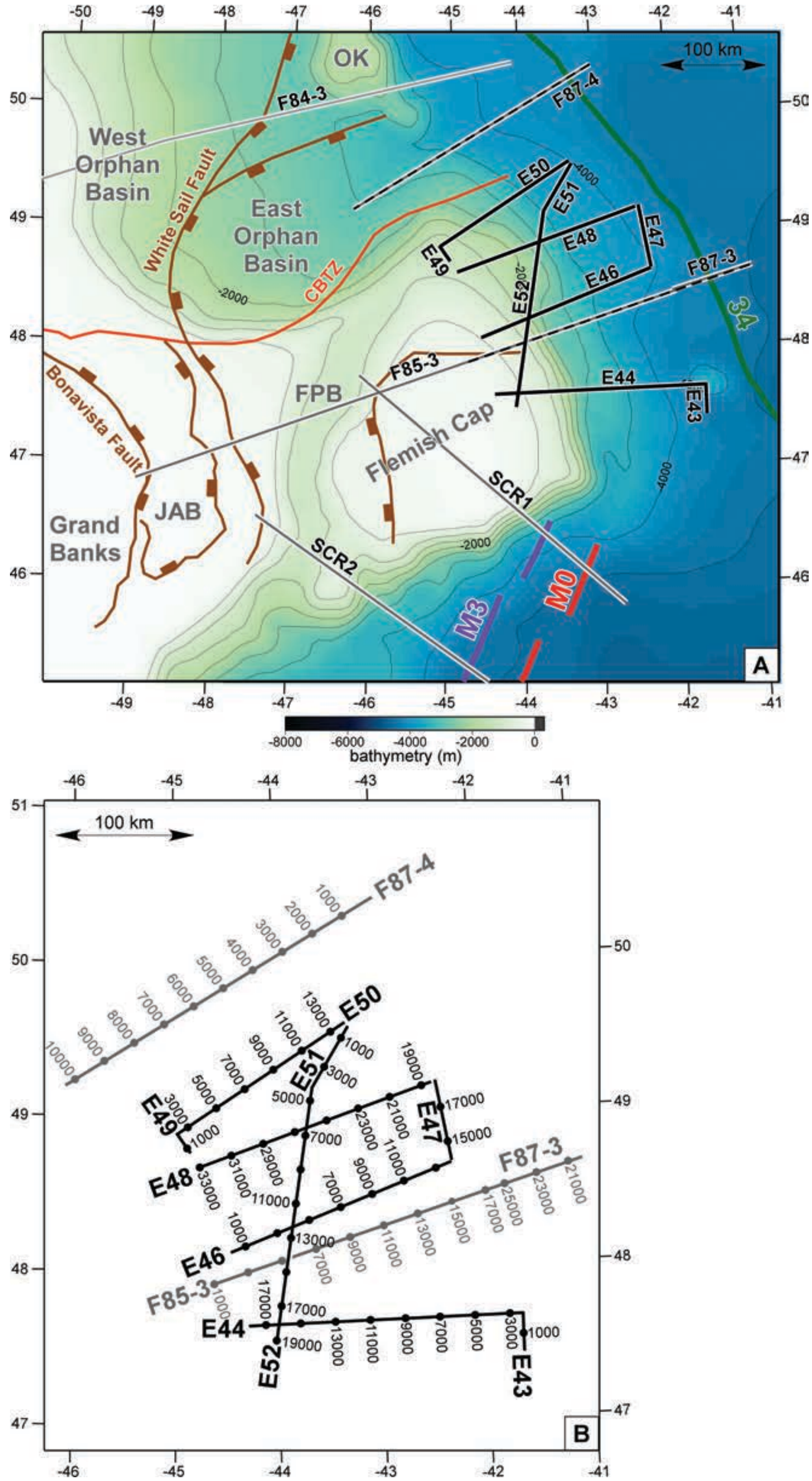

Figure 2. Detailed bathymetric map of study region (A) and a detailed plot of the specific portions of multichannel seismic reflection profiles considered in detail in this manuscript shown in (B) with regular CDP locations labelled. In (A), multichannel seismic reflection profiles are plotted with solid black lines corresponding to the Erable experiment (lines E43, E44, E46, E47, E48, E49, E50, E51 and E52) and solid grey lines corresponding to the Frontier Geoscience Project (lines F84-3, F85-3, F87-3, F87-4; Keen *et al.* 1987; Reid & Keen 1990; Chian *et al.* 1999; Louden & Chian 1999) and the SCREECH experiment (lines SCR1 and SCR2; Funck *et al.* 2003; Hopper *et al.* 2004; Shillington *et al.* 2006; van Avendonk *et al.* 2006). Portions of the FGP seismic reflection profiles considered in this study are highlighted by the dashed black lines. Locations of magnetic anomalies 34, M0 and M3 identified by Srivastava *et al.* (1988b, 2000) are plotted in (A) as green, red and purple line segments respectively. Faults and transfer zones are plotted as brown and orange lines respectively. In (B), the Erable and FGP profiles are plotted as black and grey lines, respectively. Key bathymetric features are labelled in grey. Abbreviations: CBTZ, Cumberland Belt Transfer Zone; FPB, Flemish Pass Basin; JAB, Jeanne d'Arc Basin; OK, Orphan Knoll.

then to the southeast–northwest separation of the southeastern margin of Flemish Cap from Galicia Bank (Williams 1984; Tucholke *et al.* 1989; Grant & McAlpine 1990). A final rifting phase in the Late Cretaceous (de Graciansky & Poag 1985; Tucholke *et al.* 1989; Hopper *et al.* 2006; Tucholke & Sibuet 2007) separated the northeast margins of Flemish Cap and Orphan Basin from the Goban Spur and the Porcupine High, offshore Ireland.

Orphan Basin is subdivided by the White Sail complex fault zone into an older East Orphan Basin and a younger West Orphan Basin (Enachescu *et al.* 2004c). The subbasins are characterized by a fan of faults and basement ridges varying in orientation clockwise from N–S to NE–SW (Enachescu *et al.* 2004a). The East Orphan Basin, adjacent to Flemish Cap, was subjected to the most prolonged extensional history of all of the basins on the Canadian margin lasting from the Late Triassic to the Paleocene and involving westward propagation of rifting (Enachescu *et al.* 2004c; Enachescu 2006). The initial rifting phase of the East Orphan Basin occurred during the Late Triassic to Early Jurassic and was followed by a prolonged period of subsidence. The basin was reactivated and deepened from the Late Jurassic to the Early Cretaceous while it was connected to the Jeanne d'Arc Basin to the south, the Flemish Pass Basin to the southeast and the Porcupine Basin to the north–east on the conjugate Irish Atlantic margin.

Significant overlaps between Flemish Cap and Galicia Bank in plate reconstructions of the North Atlantic margins prior to separation using large-scale plates (Le Pichon *et al.* 1977; Srivastava & Verhoef 1992) prompted the suggestion that Flemish Cap and Galicia Bank acted as microplates during rifting, moving relative to their adjacent larger plates (Le Pichon *et al.* 1977; Srivastava & Verhoef 1992; Srivastava *et al.* 2000; Sibuet *et al.* 2004). Building from this idea, Sibuet *et al.* (2007b) estimated the amount of extension experienced within the larger plates assuming the microplate model and using a new paleoreconstruction based on Bouguer gravity data. They concluded that Flemish Cap originated in the region now occupied by the Orphan Basin out of which it was rotated as a whole in a clockwise direction 43° (relative to Iberia) during the Late Triassic to Early Cretaceous and was displaced 200–300 km southeastward (relative to North America) from Late Jurassic to early Aptian time (Srivastava & Verhoef 1992; Srivastava *et al.* 2000; Enachescu 2006; Sibuet *et al.* 2007b). This hypothesized motion of Flemish Cap is thought to have involved significant transtensional movement within the East Orphan Basin, direct evidence for which has been difficult to identify on available seismic data (Enachescu 2006). Since the postulated motion of Flemish Cap preceded seafloor spreading but overlapped temporally with crustal extension and rifting between Flemish Cap/Orphan Basin and the conjugate Irish Atlantic margin, evidence for both extensional and strike-slip structures across the northeastern margin of the cap are required to support this hypothesis.

3 PAST WORK ON THE IRISH ATLANTIC MARGIN

To date, most of the existing seismic reflection and seismic refraction work on the Irish Atlantic continental margin has been concentrated on the mainland, the continental shelf and the basins therein (e.g. Porcupine Basin and Rockall Basin). Meanwhile and most relevant to this study, only a small number of studies have focused on the continent–ocean transition and these have been limited to the Goban Spur region (Peddy *et al.* 1989; Horsefield *et al.* 1994; Bullock & Minshull 2005), the conjugate margin to the northeastern margin of Flemish Cap.

A 640 km long deep seismic reflection profile, the WAM (Western Approaches Margin) line (Peddy & Hobbs 1987; Peddy *et al.* 1989), was acquired across the Goban Spur in 1985 by BIRPS (British Institutions Reflection Profiling Syndicate) and ECORS (Etude Continentale et Océanique par Réflexion et réfraction Sismiques). For these data, Peddy *et al.* (1989) interpreted a sharp continent–ocean boundary at the foot of the continental slope on the basis of drilling results from the Deep Sea Drilling Project (sites 549 and 551) which identified a thick package of volcanic rocks within 30 km of thinned continental crust. Modelling results from early coincident seismic refraction data collected along a shorter line and along two perpendicular profiles were consistent with the oceanic crust interpretation outboard of the volcanic knoll (Horsefield *et al.* 1994) but these results were poorly constrained due to the use of only one ocean-bottom seismometer (OBS) along the main profile and because that profile was unreversed. In contrast, a longer and more recently acquired coincident seismic refraction profile over the same region interpreted a 120 km wide transitional zone outboard of the volcanic basement. The landward 70 km of this zone was interpreted as exhumed serpentinized mantle peridotites (Bullock & Minshull 2005), similar to transitional crust interpreted further south on the Iberian and Newfoundland margins (Boillot *et al.* 1987; Pickup *et al.* 1996; Whitmarsh *et al.* 1996; Dean *et al.* 2000; Lau *et al.* 2006b; Sibuet *et al.* 2007a). Basement ridges, poorly constrained due to limited ray paths at the end of the modelled line, make up the 50 km wide seaward part of the transition zone and may correlate with exhumed serpentinized mantle peridotite ridges like those identified to the south on both margins (Beslier *et al.* 1993; Dean *et al.* 2000; Welford *et al.* 2010a).

4 PAST WORK ON THE NORTHEASTERN FLEMISH CAP AND ORPHAN BASIN MARGINS

Multichannel seismic reflection profiling was first undertaken along the northeastern margin of Flemish Cap in 1985 as part of the broader Frontier Geoscience Project (FGP) of the GSC in which over 6800 km of multichannel seismic reflection data were collected over the Newfoundland and Flemish Cap margins. FGP profile F85-3 (de Voogd & Keen 1987; Keen *et al.* 1987; Keen & de Voogd 1988) which extends SW–NE across the northeastern margin of the cap (Fig. 2) was later supplemented oceanward by seismic reflection profile F87-3 and an accompanying seismic refraction survey (Reid & Keen 1990). Along line F85-3, Keen & de Voogd (1988) interpreted a sharp continent–ocean crustal boundary based on the presence of a continuous landward dipping reflection corresponding to a positive magnetic anomaly. Seaward of this boundary, the seismic refraction results of Reid & Keen (1990) were consistent with the presence of oceanic crust.

In 2002, a wide-angle seismic reflection/refraction profile was acquired along the Flemish Cap Margin Transect (FLAME1; Jackson *et al.* 2002), approximately coincident with FGP profiles F85-3 and F87-3 (Fig. 2A). Results from this survey have revealed a 30 km wide transitional zone interpreted as exhumed serpentinized mantle ridges between thinned continental crust and oceanic crust, outboard of the boundary interpreted by Keen & de Voogd (1988), with serpentinized mantle with velocities of 7.4–7.9 km s^{-1} modelled at depth beneath the thinned continental crust (Gerlings *et al.* 2009). An anomalous zone with a velocity of 7.4 km s^{-1} was identified in the lower crust along a segment of profile F85-3 by Reid & Keen (1990) and was interpreted as consisting of mafic/ultramafic cumulates.

While the Orphan Basin, to the northwest of Flemish Cap, has been lightly drilled and extensively surveyed using seismic reflection techniques by the petroleum industry, few of these studies have been published in the literature and most have primarily focused on sedimentary sequences so are not directly relevant to this study. Limited crustal-scale seismic refraction surveying has been performed in the Orphan Basin (Keen & Barrett 1981; Chian *et al.* 2001) with the most recently published seismic refraction study undertaken along profile F84-3 from the GSC's FGP. The NE–SW trending profile extended from the Bonavista Platform of the Grand Banks, across the Orphan Basin to beyond Orphan Knoll, an isolated continental fragment lying inboard of the continent–ocean boundary (Chian *et al.* 2001). The resulting velocity model revealed that the Orphan Basin is underlain by stretched continental crust with velocities ranging from 6.1–7.0 km s^{-1} extending for over 400 km out to Orphan Knoll with no evidence of underplating.

5 RESULTS AND INTERPRETATION

Data acquisition for the Erable project was undertaken aboard the Canadian research ship CSS Hudson. The ship was outfitted with multichannel seismic equipment belonging to Ifremer. An array of 8 Bolt air guns with a total capacity of 92 litres was fired every 38.8 s at a cruising speed of five knots corresponding to a shot spacing of 100 m. Data were recorded by a 96 channel, 2.4 km long streamer with a 25 m receiver spacing. The resulting common-midpoint (CMP) spacing was 12.5 m and the nominal CMP fold was 12 (Srivastava & Sibuet 1992). The Erable profiles that we present were processed using similar processing flows consisting of frequency filtering, amplitude gaining, normal-moveout correction, spiking deconvolution, F–K linear noise filtering, multiple suppression (F–K filtering for the shelf, Radon transform filtering for the slope and deep water), near trace muting, stack, post-stack predictive and spiking deconvolution, trace mixing, post-stack Kirchhoff time migration and trace balancing.

We combine the processed Erable profiles considered in this manuscript into five cross-sections. These cross-sections flank and extend between the earlier FGP profiles and so both the Erable and FGP profiles are presented in order from south to north in Figs 3(A) to 9(A). The corresponding interpreted cross-sections are presented in Figs 3(B) to 9(B) and subdivide each of the lines into their inferred domains. The velocity model boundaries from the study of Reid & Keen (1990), digitized and converted to two-way traveltime, are underlain on profile F85-3 for reference (Fig. 4B).

Due to the limited coincident seismic velocity constraints currently available for the margin other than along profiles F85-3 and F87-3 (Reid & Keen 1990; Gerlings *et al.* 2009), our crustal domain interpretations were heavily based on variations in the basement morphology, depth and reflectivity as well as on the character of the imaged faulting and proximity to magnetic chron 34, interpreted as resulting from the initiation of seafloor spreading in our study region (Srivastava *et al.* 1988b).

Lacking digitized Moho depth constraints from seismic refraction surveying other than those from Reid & Keen (1990), we generated an interpreted Moho surface by running a 3-D regional gravity inversion using similar parameters to those outlined for a regional study on the Irish Atlantic continental margin (Welford *et al.* 2010b). Using the GRAV3D algorithm (Li & Oldenburg 1996, 1998), free air gravity anomalies from satellite altimetry data (Andersen *et al.* 2008) were inverted to generate a 3-D density anomaly model (relative to 2850 kg m^{-3}) over the study region (outlined in Fig. 1). The inversion was constrained by bathymetric and depth to basement information which were obtained from the GSC. The study region was discretized into a model mesh consisting of 5 km by 5 km wide by 500 m thick cells spanning 900 km in the eastings direction, 650 km in the northings direction and 35 km in depth. Density anomalies for sea water were kept fixed in the inversion while those for sediments were allowed to vary in a depth dependent way between prescribed limits (Welford *et al.* 2010b). Below basement, the inversion was given great flexibility in assigning density anomalies to reproduce the observed gravity response and no constraints were placed on which cells should correspond to crustal rocks (with density anomalies of approximately less than 170 kg m^{-3} relative to 2850 kg m^{-3}) and which prisms should correspond to upper-mantle rocks (with density anomalies of approximately greater than 170 kg m^{-3}). Since the Moho is classically defined as a seismic discontinuity and is not generally defined in terms of a specific density contrast, our interpreted Moho for the 170 kg m^{-3} isosurface represents more of a Moho proxy. It should be stressed that by using this Moho proxy, the assumption is made that Moho variations are the primary cause of subbasin mass variations rather than internal mass variations within the crust and/or mantle. From the Irish study (Welford *et al.* 2010b), the equivalently obtained Moho proxy agreed (within less than 5 km) with the Moho obtained from over 80 per cent of previous seismic refraction, seismic reflection and potential field modelling studies over the Irish margin (Kelly *et al.* 2007) and where a greater discrepancy existed, the mismatch was generally due to poor quality seismic constraints.

To relate the gravity inverted Moho proxy to the seismic time sections from this study, the Moho proxy was time-converted (using the bathymetric and sediment thickness estimates and velocities of 1500, 3000 and 6000 m s^{-1} for the water, the sediments and the crust, respectively) and is overlain as the dark grey line on Figs 3(B) to 9(B). The coarseness of this time conversion is required due to the lack of velocity constraints over the margin. Nonetheless, an average crustal velocity of 6000 m s^{-1} is consistent with the average crustal velocities resolved for thinned continental crust and oceanic crust along profiles FGP85-3 and FGP87-3 by Gerlings *et al.* (2009). As such, the overlain Moho proxy in Figs 3(B) to 9(B) should represent a reasonable estimate of Moho structure across the profiles investigated in this study with the greatest discrepancy beneath thick continental crust.

5.1 Classification of crustal domains

Rotated fault blocks, often capped with pre-rift sediments, generally characterize extended continental crust at rifted margins. In some locations, syn-rift sediments exhibiting growth towards the normal faults have also been imaged. Nonetheless, an interpretation of thinned continental crust cannot be made solely based on the presence of imaged rotated fault blocks since such features can be imaged in ultra-slow spreading ocean crust, such as the Labrador Sea (Srivastava & Keen 1995). Where available, coincident seismic velocity constraints can be used to support an interpretation of thinned continental crust since continental crustal *P*-wave velocities generally range from 5.9 to 6.8 km s^{-1} (Christensen & Mooney 1995) and exhibit a low velocity gradient (0.02 to 0.03 km s^{-1} based on an average crustal thickness of 38 km).

Typical oceanic crust is characterized by an average thickness of 7–8 km and a distinct four-layered high gradient velocity structure consisting of sediments (layer 1) with an average *P*-wave velocity of 2.0 $\mathrm{km\,s^{-1}}$, basalts and sheeted dykes (layer 2) with velocities from 3.5 to 6.6 $\mathrm{km\,s^{-1}}$, gabbro (layer 3) with velocities from 6.5 to 7.2 $\mathrm{km\,s^{-1}}$ and the upper mantle (layer 4) with an average velocity of 8.1 $\mathrm{km\,s^{-1}}$ (White 1992; Christensen & Mooney 1995). Serpentinization can reduce the velocity of layer 4 (Horen *et al.* 1996). Oceanic crust in slow spreading environments can often be recognized on seismic reflection data by its rough and highly reflective basement surface which differs from the smoother basement surface produced at fast spreading ridges (Malinverno 1991).

Transitional crust is defined as the domain between extended continental crust and oceanic crust. Four hypotheses have been proposed to explain the nature of transitional crust: (1) highly extended continental crust (Tucholke *et al.* 1989; Enachescu 1992; van Avendonk *et al.* 2006), (2) thin oceanic crust formed by slow or ultra-slow seafloor spreading (Reid 1994; Keen & de Voogd 1988; Srivastava *et al.* 2000), (3) exhumed serpentinized mantle (e.g. Boillot *et al.* 1987; Dean *et al.* 2000) and (4) a combination of any of the above (e.g. Lau *et al.* 2006b). Transitional crust attributed to exhumed serpentinized mantle has been interpreted off the Goban Spur, offshore Ireland (Bullock & Minshull 2005) and to a more limited extent off the northeastern margin of Flemish Cap (Gerlings *et al.* 2009) on the basis of seismic refraction modelling.

Extensive thinning and faulting of continental crust can lead to mantle exhumation once the extensional faults reach the base of the crust allowing sea water to penetrate the upper layer of the mantle. This sea water reacts with the mantle peridotites, hydrating the olivine to serpentine (Pérez-Gussinyé & Reston 2001; Schroeder *et al.* 2002) and changing the physical properties of the rock. Thus, serpentinization produces an increase in volume and a decrease in density, ultimately decreasing the *P*-wave velocity. With increasing degrees of serpentinization, *P*-wave velocity is further reduced producing a range of velocities for exhumed mantle that reflects the degree of serpentinization with 8.1 $\mathrm{km\,s^{-1}}$ for unaltered mantle, 7.5–7.8 $\mathrm{km\,s^{-1}}$ for 10–15 per cent serpentinization and 5 $\mathrm{km\,s^{-1}}$ for 100 per cent serpentinization (Christensen & Mooney 1995; Escartín *et al.* 2001; Schroeder *et al.* 2002; Christensen 2004). In addition, the serpentinization reaction also has a significant effect on the rheological behaviour of mantle peridotites with 10 per cent serpentine causing an abrupt reduction in strength (Escartín *et al.* 2001).

Where it has been best sampled and modelled on the Iberian and Galicia Bank margins, transitional crust generally displays a bimodal appearance containing a section of deeper basement with arguably subdued topography adjacent to a series of shallower ridges. The deeper transitional basement is characterized by a velocity structure consisting of an upper layer with low reflectivity less than 3 km thick with velocities ranging between 4.0 and 6.5 $\mathrm{km\,s^{-1}}$ (i.e. with a high velocity gradient layer) underlain by a high velocity lower layer with velocities on the order of 7.6 $\mathrm{km\,s^{-1}}$ and a low velocity gradient (Dean *et al.* 2000). Seaward, the shallower basement ridges correspond with a higher velocity range of 6.5–7.5 $\mathrm{km\,s^{-1}}$ (Dean *et al.* 2000).

5.2 Unstretched continental crust

The unstretched crust of the Flemish Cap continental shelf is imaged along most of the profiles investigated in this study, namely along lines E44 (Fig. 3), F85-3 (Fig. 4), E46 (Fig. 5), E48 (Fig. 6), E52 (Fig. 7) and E49 (Fig. 8). Along all these profiles, shallow water depth over the continental shelf combined with a hard water bottom reflection made noise from multiple reflections a severe problem. Despite the application of various multiple removal techniques, the signal-to-noise ratio remains relatively low and no clear intracrustal reflections are imaged. Nonetheless, some discrete reflectors are imaged at the base of the lower crust between 9 and 10 s on profiles E44, F85-3, E48, E49 and F87-4, between 10 and 11 s on profile E46 and between 9 and 11 s on profile E52. These lower crustal reflectors may correspond to the seismic Moho and generally correlate well with the Moho proxy from the regionally constrained 3-D gravity inversion with discrepancies possibly due to the chosen crustal velocity used in the time conversion.

5.3 Stretched continental crust

All of the seismic reflection profiles considered in this study over the northeastern margin of Flemish cap are dominated by stretched continental crust (Figs 3B to 9B). This interpretation is based on the clear presence of numerous rotated fault blocks and corresponding normal faulting of the basement, projected velocity constraints from Gerlings *et al.* (2009) and the lack of correlatable magnetic anomalies that can be attributed to seafloor spreading.

Along profile F85-3, the seaward limit of thinned continental crust interpreted by Keen and de Voogd (highlighted by the grey arrow in Fig. 4B) lies approximately 50 km inboard of the maximum extent of thinned continental crust interpreted in this study and by Gerlings *et al.* (2009). The refraction study by Reid & Keen (1990) was acquired between these two interpreted boundaries. The thinned crust in the Reid & Keen velocity model consisted of a thin layer with a velocity of 4.5 $\mathrm{km\,s^{-1}}$ at the top of the layer and a high velocity gradient. Below this layer, another thin high gradient layer was modelled with a velocity of 6.0 $\mathrm{km\,s^{-1}}$ at the top of the layer. The velocity at the top of the thick lower crust in the model had a velocity of 6.8 $\mathrm{km\,s^{-1}}$ and a low velocity gradient. Finally, an anomalous zone with a velocity of 7.4 $\mathrm{km\,s^{-1}}$ was resolved at the base of the lower crust in the landwardmost part of the model. Reid & Keen (1990) interpreted their laterally-consistent velocity model as representing oceanic crust with the anomalous lower crustal body consisting of mafic/ultramafic cumulates. The equivalent section from the velocity model of Gerlings *et al.* (2009) shows a moderately low velocity gradient from 5.7 to 6.0 $\mathrm{km\,s^{-1}}$ in the upper crust and a similar low gradient lower crust with velocities closer to 6.5 $\mathrm{km\,s^{-1}}$. The anomalous lower crustal 7.5 $\mathrm{km\,s^{-1}}$ body is also modelled by Gerlings *et al.* (2009) and is interpreted as serpentinized mantle underlying thinned continental crust. For profile F85-3 (Fig. 4), we adopt a similar interpretation to that of Gerlings *et al.* (2009). Based on the multichannel seismic reflection results, the coincident seismic refraction results and the lack of distinct magnetic anomalies, we feel that the thinned continental crust interpretation is supported by the regularity of the faulted blocks along F85-3 (Fig. 4) which differs from the chaotic faulting imaged in seafloor spreading environments with intermittent magmatism (Srivastava & Roest 1999).

Within the landward portion of stretched continental crust, all of the profiles considered in this study exhibit evidence of strike-slip faulting, from the shelf break to around 80 km seaward of it. The strike-slip motions are probably also linked with extension, making this a broad zone of transtension. While SZs appear to be broadly distributed within this interpreted zone of transtension, the interpretation is described with respect to three specific shear zones (SZ1–SZ3, Figs 3B to 9B) which may be correlatable across the profiles but which do not encompass all the shearing motion experienced along the margin. Evidence of strike-slip faulting cannot be observed directly from actual fault displacements because horizontal displacements cannot be observed on vertical images. However, secondary features can be used to infer the presence of such faults: steep fault dips, random vertical apparent offsets along adjacent faults, inversion structures and flower structures (negative for transtension). Within the inferred broad zone of strike-slip faulting on the northeastern margin of Flemish Cap, the increase in water depth from the shelf break implies significant crustal thinning which also requires an accompanying normal component of faulting. While listric normal faults within the zone of shearing are relatively rare compared with the more seaward zone, this may simply reflect insufficient depth imaging. Thus, it is suggested that most of the extension in the zone of shearing was accommodated along a combination of strike-slip and (possibly listric) steep normal faults in a transtensional environment.

SZ1 occurs at the shelf break. Profile E44 (Fig. 3C) shows a small erosion hollow at the break indicating where the main fault of the SZ subcrops on the seabed. A number of faults occur within 10 km seaward of the main fault. These faults clearly slice up the deeper-imaged sediment packages and show variable sense of throw with some possible thrusts close to the shelf-break fault. None of these faults are imaged as showing a listric form but they may merge at depth to form a negative flower structure. Farther north, the pattern changes but shows some basic similarities with that seen on profile E44. On profile F85-3 (Fig. 4B), the shelf break appears to be associated with several faults rather than just one, but the complex structures below the deeper seabed indicate a multiplicity of closely spaced faults (some of which are attributed to SZ3). Profile E46 (Fig. 5C) and profile E52 (Fig. 7C) both show steep faults defining the shelf break, with multiple steep closely spaced faults in the deeper water. Again, as on profile E44, these faults may possibly represent a negative flower structure with the faults potentially merging at depth. The clarity of SZ1 on profiles E48 (Fig. 6C) and E50 (Fig. 8C) is reduced by the burial of the earlier shelf break below younger sediments. On profile E48 (Fig. 6C), a saucer shaped depression may be contained within a negative flower structure. On profile E50 (Fig. 8C), the structure is more asymmetric as on profiles much farther to the south. Here, the main shelf-break fault shows evidence of inversion in the variable direction of growth of sediments on-lapping against the fault face.

SZ2 is best illustrated on profiles E48 (Fig. 6C) and E52 (Fig. 7B). On these profiles, there is a down-to-the-east displacement of strata across a complex steeply dipping fault zone consisting of several fault strands. Inconsistent vertical throws over time are manifest by the variable direction of growth in strata abutting the fault-zone face. Between SZ1 and SZ2 there are more steeply dipping faults with variable displacement including some probable thrusts (e.g. on profile E48). We conclude that the area, including SZ1, SZ2 and the intervening basement, is part of one broad strike-slip fault zone, characterized by steeply dipping faults of variable dip and throw, typical of strike-slip fault zones. There are also likely extensional normal faults distributed within this zone. If Flemish Cap has been rotated as suggested, the implications for how this is achieved in a body of irregular outline would include the need for a broad zone of shearing, possibly quite variable in width. Such a zone is further demonstrated by SZ3 which is observed further inboard on the southern profiles and may simply be a part of SZ1, lying close to it and taking up the strain from SZ2 which does not appear to be mapped into this southern area.

Furthest to the north in the East Orphan Basin, we include an interpretation of profile F87-4 for regional completeness as this profile has not previously been published and is regionally relevant. Extending the Erable interpretations northward is complicated by a complete lack of velocity constraints for F87-4 and the orientation of the profile along strike of much of the deformation experienced by the basin. Nonetheless, we speculate that the landward half of the profile consists of thinned continental crust, transitional crust or a combination of both based on the refraction results showing that Orphan Basin is underlain by thinned continental crust to the northwest (Chian *et al.* 2001) and the prolonged extensional history of the East Orphan Basin which may have thinned and embrittled the crust sufficiently to allow for serpentinization of the underlying mantle and ultimately the exhumation of that mantle material. On the Irish margin, extension within the Porcupine Basin is interpreted to have resulted in mantle serpentinization and localized exhumation (Reston *et al.* 2004), perhaps providing a conjugate equivalent to the evolution of the East Orphan Basin. The possible extrapolation along the bathymetric contour of SZ2 from the south complicates the picture further but does not preclude the exhumed mantle interpretation. We will revisit this issue in the discussion on transitional crust.

5.4 Oceanic crust

The onset of seafloor spreading on the northeastern margin of Flemish Cap is inferred to have occurred in the Late Cretaceous based on magnetic anomaly 34 (84 Ma) identified by Srivastava *et al.* (1988a,b). With the seaward limit of all the Erable profiles lying inboard of magnetic chron 34 (Srivastava *et al.* 1988b) and lacking any velocity constraints other than those from Gerlings *et al.* (2009) for profiles F85-3 and F87-3 (Fig. 4B), the interpretation of oceanic crust on the Erable and FGP profiles was largely based on the along-strike projection of the Gerlings *et al.* (2009) constraints and an observed change in the basement character. This change in basement character occurs oceanward of both the thinned continental crust and a series of basement highs or ridges which may correspond to serpentinized mantle. The distinct morphology of these basement highs or ridges differs from that of the faulted continental crust landward and the more irregular and reflective oceanic basement seaward.

The southernmost Erable profile considered in this study is profile E44 (Fig. 3B) which lies approximately 40 km inboard of magnetic chron 34. This profile differs significantly from the other Erable profiles in that it contains a prominent basement high that crops out through the seabed. Lacking drilling results or velocity constraints, the nature of this basement high cannot be resolved and could equally represent a volcanic seamount or a serpentinized peridotite ridge. We nonetheless prefer the volcanic seamount interpretation for two reasons. First and most importantly, the circular bathymetric morphology of the high is more consistent with that of a localized seamount rather than a ridge. Secondly, seismic refraction results to the south along SCREECH profile 1 (Funck *et al.* 2003) show no evidence for the northward continuation of the exhumed peridotite ridges identified even further south along SCREECH (Study of Continental Rifting and Extension on the Eastern Canadian Shelf) profile 2 (van Avendonk *et al.* 2006). Unfortunately, magnetic anomaly data are inconclusive in resolving whether this feature consists of exhumed mantle or oceanic crust as both types of crust as well as instances of serpentinized mantle beneath thinned continental crust can generate similar magnetic responses (Sibuet *et al.* 2007a).

If our interpretation is correct, the seamount marks the initiation of seafloor spreading on the northeastern margin of Flemish Cap, significantly earlier than the generation of magnetic chron 34. Similarly, oceanic crust is interpreted approximately 60 km inboard of magnetic chron 34 along the other FGP and Erable profiles investigated in this study. On the Goban Spur margin, oceanic crust is also interpreted inboard of magnetic chron 34 (Bullock & Minshull 2005).

5.5 Transitional crust

Along profile F85-3 (Fig. 4B), a 25 km wide zone of subtle basement ridges has been interpreted as exhumed serpentinized mantle by Gerlings *et al.* (2009) on the basis of seismic refraction modelling. Accepting this interpretation and extending it off the line, a similar set of ridges can be observed immediately to the northwest along profile E46 (CDPs 12200–13700 in Fig. 5B) and possibly further to the northwest along profiles E48, E50 and E51 (CDPs 22000–23000 in Fig. 6B, CDPs 800–2500 in Fig. 7B and CDPs 11900–13200 in Fig. 8B). Together, the interpreted ridges define a narrow zone of exhumed mantle that extends along most of the northeastern margin of Flemish Cap and separates thinned continental crust from oceanic crust. On the southernmost profile considered in this study, E44 (Fig. 3B), the only structure that could be interpreted as a ridge more closely resembles a classic volcanic seamount due to its circular morphology and limited along strike extent. Meanwhile, to the northwest into the East Orphan Basin, the exhumed mantle ridges interpretation can be projected to profile F87-4 (Fig. 9B) but there is great uncertainty as to its lateral extent. Dividing profile F87-4 on the basis of basement morphology and basement reflectivity alone, we interpret a 50 km wide zone of exhumed mantle ridges between CDPs 3400 and 5700 (Fig. 9B) but this interpretation could easily be extended landward to encompass the rest of the profile. The orientation of the profile along strike of the East Orphan Basin complicates the interpretation as the basement structures are not clearly imaged. That coupled with the extensive extensional history of the basin make both interpretations equally plausible. Future seismic refraction surveys or drilling of basement within the basin are necessary to elucidate the true nature of the basement in the East Orphan Basin.

6 DISCUSSION

6.1 Regional distribution of crustal domains and faulting

The interpreted crustal domains from the individual Erable profiles are plotted on a regional bathymetry map in Fig. 10 along with corresponding interpretations for nearby FGP profiles. The interpolated interpretations provide a regional view of the distribution of crustal domains over the northeastern margin of Flemish Cap. In comparison with a similar map generated for the southeastern Newfoundland and Flemish Cap margins (fig. 10 in Welford *et al.* 2010a), elements of which have been included in Fig. 10, the northeastern margin of Flemish Cap appears to be somewhat simpler.

A zone of stretched continental crust exists along the entire northeastern margin of Flemish Cap ranging in width from approximately 100 km in the south (Fig. 3B) to approximately 120 km in the north (Fig. 8B). Within this zone of extended continental crust, a region that may have experienced strike-slip shearing is identified on the basis of interpreted strike-slip structures that can be correlated across the seismic lines as distinct shear zones (SZ1, SZ2 and SZ3). Overall, the width of this zone of inferred shearing expands from approximately 40 km in the south (Fig. 3B) to 50 km in the north (Fig. 8B) with a change in the character in the inferred zone of strike-slip shearing occurring between profiles F85-3 and E46. This abrupt change corresponds with a transfer zone identified by Srivastava *et al.* (1988a) on the basis of aeromagnetic data. A second transfer zone identified by Srivastava *et al.* (1988a) lies between profile 49-50 (Fig. 8B) and profile F87-4 (Fig. 9B). While these transfer zones clearly affected outboard seafloor magnetic anomalies younger than chron 33, it is possible, as interpreted on the southeastern margins of the Grand Banks and Flemish Cap (Welford *et al.* 2010a), that the transfer zones resulted from inherited along-strike heterogeneities in the continental crust which ultimately resulted in the along-strike variations in rifting style observed along the northeastern margin of Flemish Cap. The presence of these inferred transfer zones also makes extrapolation of SZ2 into the zone of strike-slip shearing interpreted along profile F87-4 questionable.

The combined strike-slip SZs and extensional faulted structures along the profiles investigated in this study are in good agreement with results from analogue modelling of crustal faulting under transtension (Schreurs & Colletta 1998). In such models, shearing is first accommodated by the development of en echelon vertical strike-slip faults at low angles to the main direction of shear. As deformation continues, normal faults trending parallel to the older strike-slip faults develop between them and partition the fault movement and gravitational failure (Schreurs & Colletta 1998). The temporal partitioning of faulting under a constant transtensional regime can explain the bimodal faulting distribution on the northeastern margin of Flemish Cap and supports the idea that the Flemish Cap was subjected to both shearing and extension at or near the same time.

A narrow 25 km wide zone of transitional crust is interpreted along most of the Erable profiles considered in this study and is interpreted to consist of exhumed serpentinized mantle ridges on the basis of limited velocity constraints from Gerlings *et al.* (2009) and consistent basement morphology across the reflection profiles. The zone of transitional crust may widen to 50 km or more to the northwest of Flemish Cap into the East Orphan Basin along profile F87-4 but this interpretation is poorly constrained by the available seismic data.

The onset of seafloor spreading and the generation of oceanic crust is interpreted to have been initiated first along profile E43-44 (Fig. 3B) to the east of Flemish Cap before becoming parallel to the northeast margin of Flemish Cap as evidenced along the remaining Erable and FGP profiles. The paucity of exhumed mantle and the earlier onset of seafloor spreading interpreted along profile E43-44 (Fig. 3B) and along profile SCR1 (Funck *et al.* 2003) to the south (Fig. 10) may somehow be related to their proximity to the triple junction which was responsible for the opening of the Bay of Biscay to the east and where the direction of rifting flipped from NW–SE along the southeastern margin of Flemish Cap to SW–NE along the northeastern margin of Flemish Cap. This triple junction was active immediately prior to magnetic chron 34 (Williams 1975; Kristoffersen 1978; Sullivan 1983). Results from numerical modelling studies of similar triple junctions suggest a focusing of higher temperatures and increased mantle upwelling along the slowest-spreading ridge toward the triple junction (Georgen & Lin 2002; Georgen 2008) which may have increased the melt supply enough so as to have prevented mantle exhumation prior to seafloor spreading in proximity to profile E43-44.

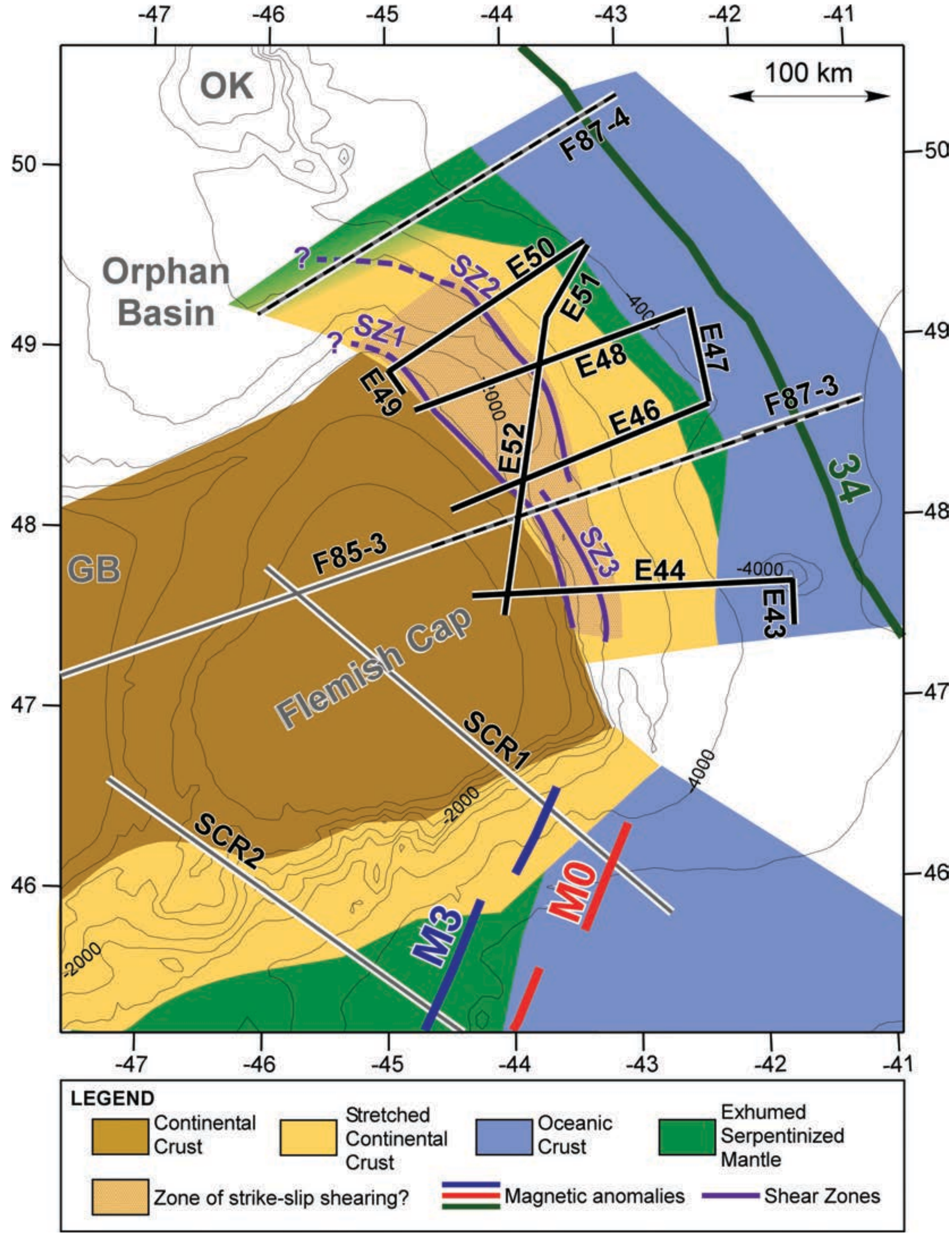

Figure 10. Map of project area showing bathymetry (grey contours) and the interpreted crustal boundaries and domains from the Erable and FGP profiles considered in this study and that of Welford *et al.* (2010a) with seismic line descriptions as in the caption of Fig. 2. The location of magnetic anomaly 34 is taken from Srivastava *et al.* (1988b). The purple lines correspond to the SZs interpreted along the Erable and FGP profiles that separate zones with different crustal thinning styles. Abbreviations: GB, Grand Banks; OK, Orphan Knoll.

6.2 Along-strike variations in rifting style

Variations in the amount of extension experienced along-strike of a given margin can be indicative of variations in rifting style. To quantify these variations, the cumulative offset and displacement across well imaged faults can be calculated on good quality seismic reflection data. Alternatively, crustal-scale models derived from seismic refraction or other geophysical techniques can be used (e.g. Reston 2007). Since the quality of fault imaging along the older vintage Erable profiles from this study was not sufficient for a quantitative fault analysis, extension across the northeastern margin of Flemish Cap was investigated using potential field methods.

Total crustal thickness was computed across our study area using the Moho proxy obtained from a regional 3-D gravity inversion (described above) and the bathymetric and sediment thickness estimates used to constrain that inversion. The resulting crust was found to be highly variable in thickness with the thinnest crust (8 km) beneath the East and West Orphan basins and the thickest crust

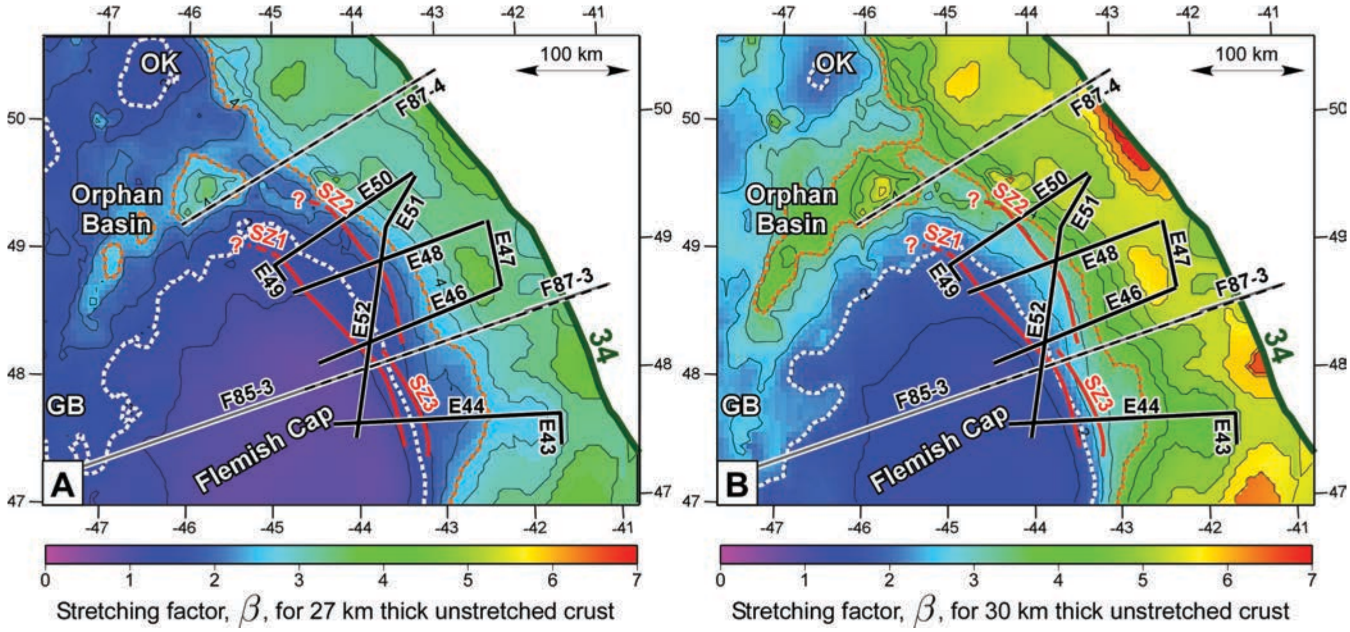

Figure 11. Maps of project area showing stretching factors, β, computed using unstretched crustal thicknesses of 27 km (A) and 30 km (B). Regions corresponding to oceanic crust, outboard of magnetic anomaly 34 (Srivastava *et al.* 1988b), have been masked out from both maps. On both plots, the $\beta = 2$ contour, corresponding to the stretching factor above which polyphase faulting becomes important (Reston 2007), and the $\beta = 3.5$ contour, corresponding to the stretching factor above which embrittlement of the entire crust is possible (Pérez-Gussinyé & Reston 2001; Pérez-Gussinyé *et al.* 2003), are highlighted by the white and orange dotted lines, respectively. Labelled seismic lines as in the caption of Fig. 2. The red lines correspond to the SZs interpreted along the Erable and FGP profiles that separate zones with different crustal thinning styles. Abbreviations: GB, Grand Banks; OK, Orphan Knoll.

(27 km) beneath Flemish Cap. Thinning was also found to be most abrupt and dramatic oceanward (compared to toward Orphan Basin) with over 60 per cent thinning occurring within a span of less than 100 km. The seawardmost major SZs interpreted along the individual Erable seismic reflection lines (SZ2 and SZ3) roughly correspond to a 65 per cent thinning of the crust while inboard, shear zone SZ1 roughly corresponds to a 50 per cent thinning.

An independent estimate of 30 km for the thickness of the unstretched crust of Flemish Cap was obtained by Funck *et al.* (2003) from modelling of wide-angle reflection/refraction seismic data. Using the 27 and 30 km estimates for the thickness of unextended continental crust from this study and from Funck *et al.* (2003), we have constructed maps of extension/stretching factor, β, across the margin (Fig. 11). The extension factor, which corresponds to the ratio of extended length to unextended length, was computed by taking 1 km-long 2-D blocks of both 27 and 30 km thick crust, determining the corresponding extended lengths for the varying crustal thicknesses in the study region (assuming that the cross-sectional area remains constant) and plotting their ratios. This highly simplified approach to computing extension factors will produce less conclusive estimates if along-strike transport has been significant along the margin (as we postulate that it has) but can nonetheless be used to provide a first-order view of rifting trends.

The plots of stretching factors across the study area for both 27 and 30 km thick unextended crust (Figs 11A and B) show the same general trends. The inner continental slopes of the combined Flemish Cap and Orphan Basin margins are characterized by an average stretching factor of approximately 2. This value is in close agreement with that suggested by Sibuet *et al.* (2007b) based on their reconstruction using regional Bouguer gravity data. Oceanward, toward magnetic anomaly 34, the inferred onset of seafloor spreading (Srivastava *et al.* 1988b), stretching factors increase to between 4 and 7. The one exception to this trend is the East Orphan Basin where large stretching factors are also observed.

Highlighted on the plots in Fig. 11 are two key contours. The first, where $\beta = 2$ and indicated by the dotted white line, corresponds to the stretching factor above which polyphase faulting becomes important and older faulting can be obscured by younger faulting making it difficult to quantify the total amount of extension based on seismically imaged faults alone (Reston 2007). On the northeastern margin of Flemish Cap, this contour corresponds well with the landwardmost SZ1 interpreted along the Erable profiles in this study (Figs 3A to 8A) and demonstrates that even with improved imaging of the faults along the Erable profiles, extension factors computed from them would underestimate the amount of crustal thinning.

In Fig. 11, the second contour, where $\beta = 3.5$ and indicated by the dotted orange line, corresponds to the stretching factor above which embrittlement of the entire crust is thought to be possible based on numerical modelling studies (Pérez-Gussinyé & Reston 2001; Pérez-Gussinyé *et al.* 2003). Total crustal embrittlement can result in the serpentinization of the upper mantle along faults that cross-cut the entire crust. The localization of the higher stretching factors in both plots of Fig. 11 agrees well with the seismic refraction modelling results from Reid & Keen (1990) and preliminary results from Gerlings *et al.* (2009) along profiles F85-3 and F87-3 (Fig. 4B) where serpentinized mantle has been interpreted beneath the thinned continental crust. Stretching factors greater than 3.5 computed for the East Orphan Basin, whether limited to discontinuous pockets or a continuous zone, would suggest that embrittlement of the entire crust and possible upper-mantle serpentinization may have played a role in its evolution, possibly focused at depth by a splay of the White Sail Fault. Both plots in Fig. 11 lend support to the exhumed mantle interpretation of most of the landward end of seismic reflection profile F87-4 (Fig. 9B). To date, there are no seismic or drilling data on this margin showing evidence of exhumation at the surface of any serpentinized mantle material as has been interpreted on the conjugate Goban Spur margin (Bullock & Minshull 2005) and within the Porcupine Basin (Reston *et al.* 2004) but this may simply be due to the lack of sampling.

6.3 Reconstruction and rifting evolution model

In Fig. 12, the interpreted crustal domains from this study and from earlier work in the Orphan Basin (Chian *et al.* 2001) and on the conjugate Irish Atlantic margin (Makris *et al.* 1988; Hauser *et al.* 1995; Bullock & Minshull 2005) are plotted on a paleoreconstruction of the margins at magnetic chron 34 (84 Ma) adapted from Srivastava *et al.* (1988b). Superimposed structural components on the map were adapted from the structural map presented by Sibuet *et al.* (2007b) and originally modified from Enachescu *et al.* (2004a,b,c). This map reveals a number of interesting features.

The Flemish Cap and Goban Spur conjugate margins form an asymmetrical pair. While an extensive 120 km wide zone of transitional crust, interpreted as exhumed serpentinized mantle has been identified off Goban Spur (Bullock & Minshull 2005), the equivalent transitional zone interpreted as exhumed serpentinized mantle on the northeastern margin of Flemish Cap is significantly narrower at 25 km (Gerlings *et al.* 2009). To the northwest, at the opening of the Porcupine Basin, comparisons across the conjugate pair are complicated by the poor quality and vintage of the seismic constraints on the Irish Atlantic margin (Makris *et al.* 1988). There is however inferred evidence for exhumed serpentinized mantle

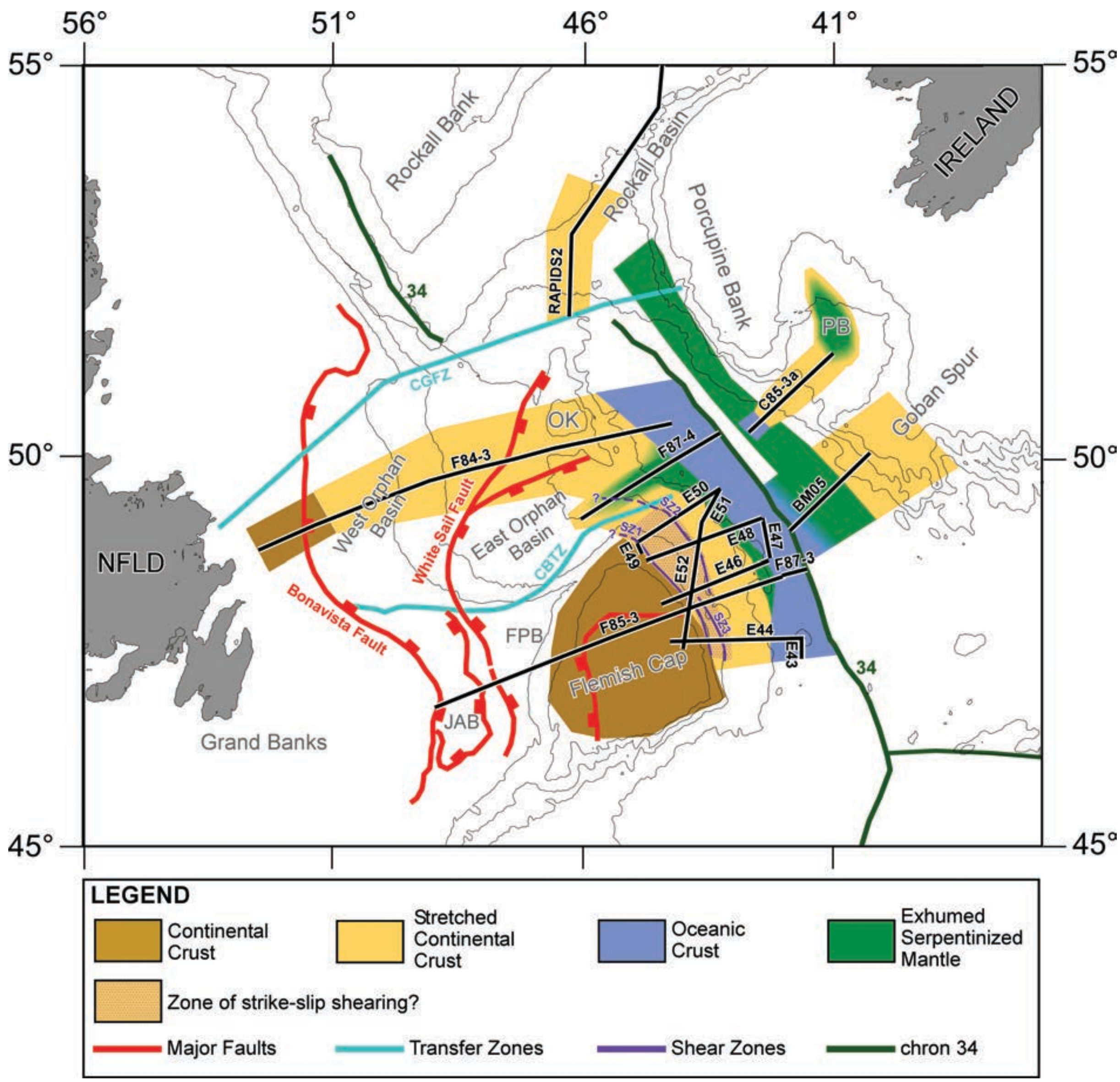

Figure 12. Interpreted crustal domains from this study, from a regional 3-D gravity inversion over the Irish margin (Welford *et al.* 2010b) and from seismic profiles F84-3 (Chian *et al.* 2001), BM05 (Bullock & Minshull 2005), C85-3a (Makris *et al.* 1988) and RAPIDS2 (Hauser *et al.* 1995) superimposed on a reconstruction of the Newfoundland and Irish conjugate margins at magnetic anomaly 34 adapted from Srivastava *et al.* (1988b). All seismic profiles are plotted as solid black lines outlined in white. Superimposed structural components on the map were adapted from the structural map presented by Sibuet *et al.* (2007b) and originally modified from Enachescu *et al.* (2004a,b,c). The purple lines correspond to the SZs interpreted along the Erable and FGP profiles that separate zones with different crustal thinning styles. Abbreviations: CBTZ, Cumberland Belt Transfer Zone; CGFZ, Charlie Gibbs Fracture Zone; FPB, Flemish Pass Basin; JAB, Jeanne d'Arc Basin; NFLD, Newfoundland; OK, Orphan Knoll; PB, Porcupine Basin.

within the Porcupine Basin from seismic reflection data and gravity modelling (Reston *et al.* 2004) and both outboard of the Porcupine High and within the Porcupine Basin from recent gravity inversion studies of the Irish margin (Welford *et al.* 2010b). Similarly, Chian *et al.* (2001) suggested that exhumed serpentinized mantle could be present outboard of Orphan Knoll along profile F84-3 but they were not able to provide any conclusive evidence due to poor seismic constraints. Should there prove to be mirrored instances of exhumed serpentinized mantle outboard of Orphan Knoll and the Porcupine High, symmetry in the late stages of rifting could be inferred.

The amount of evidence for the hypothesized rotation and southward displacement of Flemish Cap out of Orphan Basin is mounting (Enachescu *et al.* 2005; Sibuet *et al.* 2007b; Gacal-Isler 2009) and the results from this study are supportive of this hypothesis. With both extensional and strike-slip structures observed along all of the profiles investigated in this study, it is clear that the northeastern margin of Flemish Cap was affected by two major tectonic processes acting in tandem.

The temporal evolution of the Flemish Cap and its margins that we envision is shown in Fig. 13 as a simplified schematic cartoon.

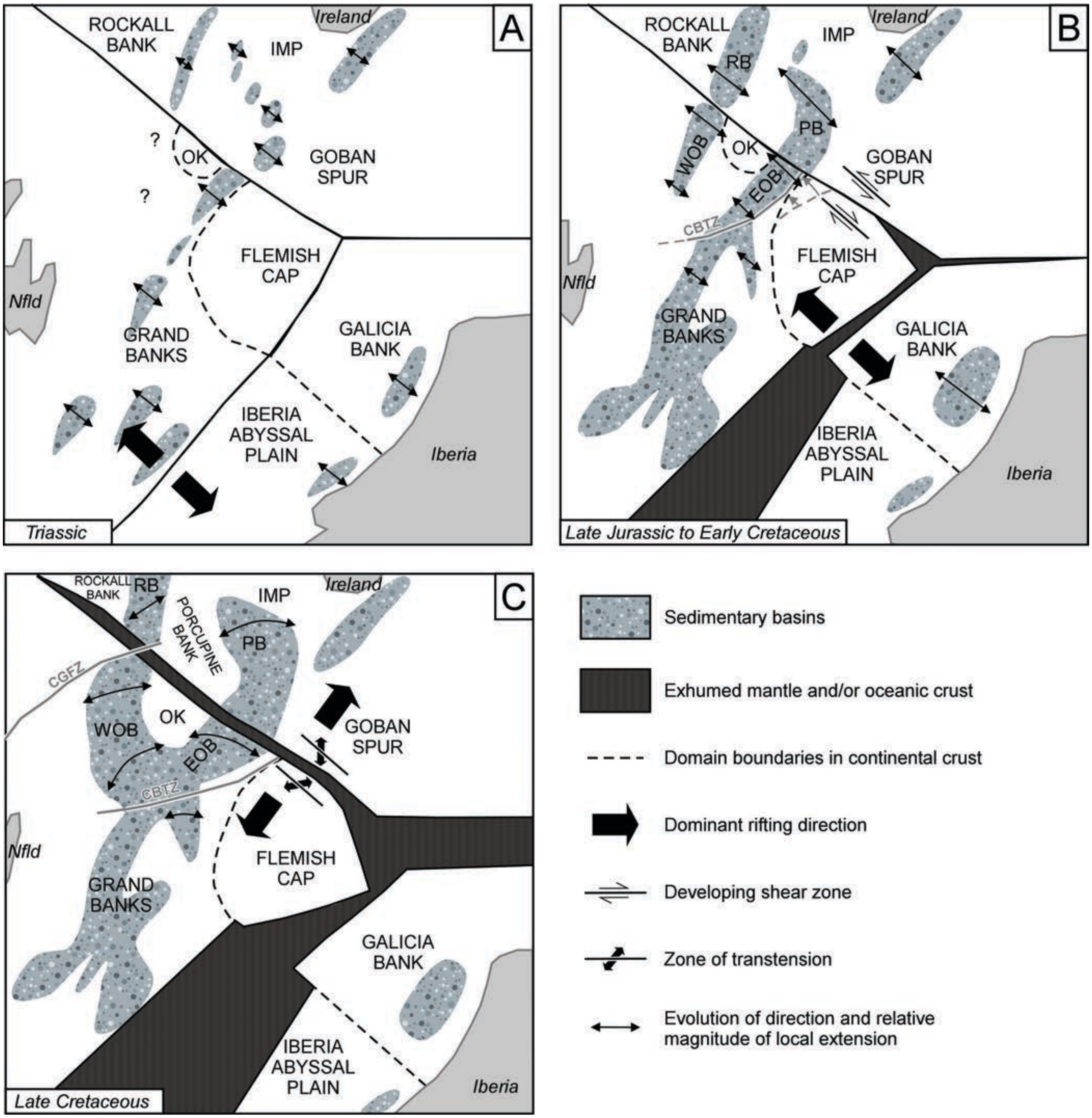

Figure 13. Simplified schematic cartoon of the temporal evolution of the Newfoundland, Irish and Iberian margins and their sedimentary basins from the Triassic (A), through the Late Jurassic and Early Cretaceous (B), to the Late Cretaceous (C). Abbreviations: CBTZ, Cumberland Belt Transfer Zone; CGFZ, Charlie Gibbs Fracture Zone; EOB, East Orphan Basin; IMP, Irish Mainland Platform; Nfld, Newfoundland; OK, Orphan Knoll; PB, Porcupine Basin; RB, Rockall Basin; WOB, West Orphan Basin.

Rifting during the Triassic was oriented NW–SE and resulted in the development of distinct NE–SW trending basins on the Grand Banks, in the East Orphan Basin and on both the Irish and Iberian margins (Fig. 13A). While Triassic sediments have been inferred in the early Rockall Basin (Naylor & Shannon 2009), basin development in the Triassic within the West Orphan Basin cannot be verified due to a lack of deep well control. From the Late Jurassic to the Early Cretaceous, rifting continued to propagate northward and was slowly replaced by seafloor spreading (Fig. 13B). The continued rifting enlarged pre-existing basins on the Grand Banks and Iberian margins and resulted in the creation of a series of interconnected basins all the way up onto the Irish margin. Separation of the southeastern margin of Flemish Cap from Galicia Bank was delayed relative to the margins further to the south with seafloor spreading beginning at around magnetic anomaly M0 (120 Ma) in the Early Cretaceous (Boillot *et al.* 1987). This delayed separation was possible because much of the NW–SE extension that occurred from the Late Jurassic to Early Cretaceous (Williams 1984; Tucholke *et al.* 1989; Grant & McAlpine 1990) was accommodated to the North American continental side of Flemish Cap in the East and West Orphan basins. While the northeastern margin of Flemish Cap remained relatively fixed during this period, it may have experienced some degree of strike-slip shearing. When the rifting propagated northward and became oriented NE–SW in the Late Cretaceous (de Graciansky & Poag 1985; Tucholke *et al.* 1989; Hopper *et al.* 2006; Tucholke & Sibuet 2007), the East Orphan Basin was again reactivated and widened with structures forming perpendicular to this new direction of extension (Fig. 13C). This enlargement and reorganization within the East Orphan Basin caused the formation of curved faults and basement ridges within the basin. On the northeastern margin of Flemish Cap, this change in rifting orientation would have superimposed a NE–SW extensional component on the pre-existing strike-slip regime, ultimately subjecting the margin to transtension. On the Irish margin, the change in rifting orientation resulted in enhanced NE–SW rifting within the Porcupine Basin. Supposing that the eastern limit of the zone of strike-slip shearing inferred from the Erable results did connect through profile F87-4 to the eastern splay of the White Sail Fault and that the western limit corresponded to the Cumberland Transfer Zone identified by Enachescu (1987), these structures may provide some of the first evidence for the development of arcuate fault systems in a transtensional rifting environment.

7 CONCLUSIONS

Interpreted multichannel seismic reflection profiles from the 1992 Erable experiment across the northeastern margin of Flemish Cap reveal evidence for both strike-slip shearing and normal faulting within thinned continental crust as well as a narrow zone of transitional crust between the thinned continental crust and oceanic crust. Combined with results from earlier geophysical surveys, interpolation of the interpreted crustal domains across the study region reveals:

(i) A zone of thinned continental crust varying in width from 100 to over 120 km along the entire northeastern margin of Flemish Cap.

(ii) Evidence for a 40 to 50 km wide zone of strike-slip shearing within the zone of thinned continental crust.

(iii) A pattern of combined extensional and strike-slip structures consistent with strain partitioning under transtension as observed from analogue modelling studies.

(iv) A narrow 25 km wide zone of transitional crust interpreted as exhumed serpentinized mantle ridges along most of the margin.

(v) A consistent onset of seafloor spreading prior to magnetic chron 34 (84 Ma) along the entire margin.

(vi) A distinct asymmetry in the structures across the northeastern margin of Flemish Cap and the Goban Spur on the conjugate Irish Atlantic margin, likely due to independent motion of Flemish Cap out of the plane of extension.

(vii) Evidence for embrittlement of the entire crust in the East Orphan Basin possibly accompanied by serpentinization of the upper mantle and mantle exhumation.

The superposition of interpreted extensional and strike-slip structures within the stretched continental crust of the northeastern margin of Flemish Cap is consistent with the postulated rotation and displacement of Flemish Cap out of Orphan Basin. The extrapolation of major structural features which delimit the boundaries of East Orphan Basin into the sheared zone identified along the northeastern margin of Flemish Cap may provide evidence for the development of arcuate fault systems in a transtensional rifting environment. Variations in the distribution and style of continental rifting and shearing may have been influenced by ancient transfer zones inherited from pre-existing lithospheric heterogeneities along strike of the margin.

ACKNOWLEDGMENTS

We would like to thank the Geological Survey of Canada and Ifremer for funding the Erable cruise on the CSS Hudson. We would also like to thank the Natural Sciences and Engineering Research Council of Canada for funding in support of this research (NSERC-PDF to Welford and Discovery Grant to Hall). The Atlantic Innovation Fund also provided support to the PanAtlantic Petroleum Systems Consortium (PPSC) which contributed to some of the postdoctoral salary support. We thank Tim Henstock and Dale Sawyer for constructive and encouraging reviews.

REFERENCES

Andersen, O., Knudsen, P., Berry, P., Freeman, J., Pavlis, N. & Kenyon, S., 2008. The DNSC08 ocean wide altimetry derived gravity field, in *Proceedings of the EGU 2008 Meeting Programme,* Vienna, Abstract EGU2008-A-07163; G1-1MO1O-003, European Geosciences Union.

Beslier, M., Ask, M. & Boillot, G., 1993. Ocean-continent boundary in the Iberia Abyssal Plain from multichannel seismic data, *Tectonophysics,* **218,** 383–393.

Boillot, G. *et al.*, 1987. Tectonic denudation of the upper mantle along passive margins: a model based on drilling results (ODP leg 103, western Galicia margin, Spain), *Tectonophysics,* **132**(4), 335–342.

Bullock, A.D. & Minshull, T.A., 2005. From continental extension to seafloor spreading: crustal structure of the Goban Spur rifted margin, southwest of the UK, *Geophys. J. Int.,* **163,** 527–546.

Chian, D., Louden, K.E., Minshull, T.A. & Whitmarsh, R.B., 1999. Deep structure of the ocean-continent transition in the southern Iberia Abyssal Plain from seismic refraction profiles: ocean drilling program (Legs 149 and 173) transect, *J. geophys. Res.,* **104**(B4), 7443–7462.

Chian, D., Reid, I. & Jackson, H., 2001. Crustal structure beneath Orphan Basin and implications for nonvolcanic continental rifting, *J. geophys. Res.,* **106**(B6), 10 923–10 940.

Christensen, N., 2004. Serpentinites, peridotites, and seismology, *Int. Geol. Rev.,* **46**(9), 795–816.

Christensen, N. & Mooney, W., 1995. Seismic velocity structure and composition of the continental crust, *J. geophys. Res.,* **100,** 9761–9788.

de Graciansky, P. & Poag, C., 1985. Geologic history of Goban Spur, northwest Europe continental margin, in *Initial Reports of the DSDP,* Vol. 80, chapter 58, pp. 1187–1216, edsde Graciansky P. & Poag, C., US Government Printing Office, Washington, DC.

de Voogd, B. & Keen, C., 1987. Lithoprobe east: results from reflection profiling of the continental margins: Grand Banks region, *Geophys. J. R. astr. Soc.,* **89**(1), 195–200.

Dean, S., Minshull, T., Whitmarsh, R. & Louden, K., 2000. Deep structure of the ocean-continent transition in the southern Iberia Abyssal Plain from seismic refraction profiles: the IAM-9 transect at 40 20'N, *J. geophys. Res.,* **105,** 5859–5886.

Deemer, S., Hall, J., Solvason, K., Lau, K.H., Louden, K.E., Srivastava, S. & Sibuet, J.-C., 2009. Structure and development of the southeast Newfoundland continental passive margin: derived from SCREECH Transect 3, *Geophys. J. Int.,* **178**(2), 1004–1020.

Enachescu, M.E., 1987. Tectonic and structural framework of the northeast Newfoundland continental margin, in *Sedimentary Basins and Basin-Forming Mechanisms,* Vol. 12, pp. 117–146, eds Beaumont C. & Tankard, A., Canadian Society of Petroleum Geologists, Calgary, Alberta.

Enachescu, M.E., 1992. Basement extension on the Newfoundland continental margin (Canadian east coast), in *International Basement Tectonics Association Publication no. 7,* pp. 227–256, ed. Mason, R., Kluwer, Dordrecht.

Enachescu, M.E., 2006. Structural setting and petroleum potential of the Orphan Basin, offshore Newfoundland and Labrador, *Recorder,* **31**(2), 5–13.

Enachescu, M.E., Hogg, J. & Meyer, K., 2004a. East Orphan Basin, offshore Newfoundland and Labrador: a deep water super extended rift with potential petroleum system, in *Canadian Society of Petroleum Geologists (CSPG) Annual Convention*, Expanded Abstracts, Canadian Society of Petroleum Geologists, Calgary, Alberta.

Enachescu, M.E., Kearsey, S., Hogg, J., Einarsson, P., Nader, S. & Smee, J., 2004b. Orphan Basin, offshore Newfoundland, Canada: structural and tectonic framework, petroleum systems and exploration potential, *in Proceedings of the Society of Exploration Geophysicists (SEG) 74th Annual Meeting and Exposition*, Expanded Abstracts, **23**(382), Denver, CO.

Enachescu, M.E., Meyer, K. & Hogg, J., 2004c. East Orphan Basin: structural setting and evolution with seismic and potential field arguments, in *Proceedings of the Canadian Society of Exploration Geophysicists (CSEG) Annual Convention*, Expanded Abstracts, Canadian Society of Petroleum Geologists, Calgary, Alberta.

Enachescu, M.E. *et al.*, 2005. Evolution and petroleum potential of Orphan Basin, offshore Newfoundland, and its relation to the movement and rotation of Flemish Cap based on plate kinematics of the North Atlantic, in *Proceedings of the Petroleum Systems of Divergent Continental Margin Basins, 25th Annual GCSSEPM Foundation – Bob F. Perkins Research Conference*, Houston, TX.

Escartín, J., Hirth, G. & Evans, B., 2001. Strength of slightly serpentinized peridotites: implications for the tectonics of oceanic lithosphere, *Geology,* **29**(11), 1023–1026.

Funck, T., Hopper, J.R., Larsen, H.C., Louden, K.E., Tucholke, B.E. & Holbrook, W.S., 2003. Crustal structure of the ocean-continent transition at Flemish Cap: seismic refraction results, *J. geophys. Res.,* **108**(B11), doi:10.1029/2003JB002434.

Gacal-Isler, B., 2009. Mesozoic tectonic and stratigraphic evolution of the Orphan Basin, with special emphasis on regional correlations with Flemish Pass and Northern Jeanne d'Arc basins, Grand Banks of Newfoundland, *MSc thesis*, Memorial University of Newfoundland, Canada.

Georgen, J., 2008. Mantle flow and melting beneath oceanic ridge-ridge-ridge triple junctions, *Earth planet. Sci. Lett.,* **270,** 231–240.

Georgen, J. & Lin, J., 2002. Three-dimensional passive flow and temperature structure beneath oceanic ridge-ridge-ridge triple junctions, *Earth planet. Sci. Lett.,* **204,** 115–132.

Gerlings, J., Louden, K.E. & Jackson, H.R., 2009. The crustal structure of the Flemish Cap continental margin (E Canada): new evidence for asymmetric rifting from Goban Spur (NW Europe), *EOS, Trans. Am. geophys. Un.,* 90(52), Fall Meeting Supplement, Abstract T31C-1847.

Grant, A. & McAlpine, K., 1990. The continental margin around Newfoundland, in *Geology of the Continental Margin of Eastern Canada,* chapter 6, pp. 239–292, eds Keen, M. & Williams, G., Geological Survey of Canada, Geology of Canada, no.2.

Hauser, F., O'Reilly, B.M., Jacob, A.B., Shannon, P.M., Makris, J. & Vogt, U., 1995. The crustal structure of the Rockall Trough: differential stretching without underplating, *J. geophys. Res.,* **100**(B3), 4097–4116.

Haworth, R. & Keen, C.E., 1979. The Canadian Atlantic margin: a passive continental margin encompassing an active past, *Tectonophysics,* **59,** 83–126.

Hopper, J., Funck, T., Tucholke, B., Larsen, H.C., Holbrook, W.S., Louden, K.E., Shillington, D.J. & Lau, H., 2004. Continental breakup and the onset of ultraslow seafloor spreading off Flemish Cap on the Newfoundland rifted margin, *Geology,* **32**(1), 93–96.

Hopper, J., Funck, T., Tucholke, B., Louden, K., Holbrook, W. & Larsen, H.C., 2006. A deep seismic investigation of the Flemish Cap margin: implications for the origin of deep reflectivity and evidence for asymmetric break-up between Newfoundland and Iberia, *Geophys. J. Int.,* **164**(3), 501–515.

Horen, H., Zamora, M. & Dubuisson, G., 1996. Seismic waves velocities and anisotropy in serpentinized peridotites from Xigaze ophiolite: abundance of serpentine in slow spreading ridge, *Geophys. Res. Lett.,* **23**(1), 9–12.

Horsefield, S.J., Whitmarsh, R.B., White, R.S. & Sibuet, J.-C., 1994. Crustal structure of the Goban Spur rifted continental margin, NE Atlantic, *Geophys. J. Int.,* **119,** 1–19.

Jackson, R., Asprey, K., Chapman, B., Goold, S., Girouard, P., Johnston, L. & Louden, K., 2002. *Hudson 2002-2011 Cruise report Flemish Cap Margin Transect*, Open file # 1234, Geological Survey of Canada, Natural Resources Canada.

Keen, C. & de Voogd, B., 1988. The continent-ocean boundary at the rifted margin of eastern Canada: new results from deep seismic reflection studies, *Tectonics,* **7,** 107–124.

Keen, C.E. & Barrett, D., 1981. Thinned and subsided continental crust on the rifted margin of eastern Canada: crustal structure, thermal evolution and subsidence history, *Geophys. J. R. astr. Soc.,* **65,** 443–465.

Keen, C.E., Boutilier, R., de Voogd, B., Mudford, B. & Enachescu, M.E., 1987. Crustal geometry and extensional models for the Grand Banks, eastern Canada: constraints from deep seismic reflection data, in *Sedimentary Basins and Basin-Forming Mechanisms,* Vol. 12, pp. 101–115, eds Beaumont, C. & Tankard, A., Canadian Society of Petroleum Geologists, Calgary, Alberta.

Kelly, A., England, R.W. & Maguire, P.K., 2007. A crustal seismic velocity model for the UK, Ireland and surrounding seas, *Geophys. J. Int.,* **171,** 1172–1184.

King, L., Fader, G., Poole, W. & Wanless, R., 1985. Geological setting and age of the Flemish Cap granodiorite, east of the Grand Banks of Newfoundland, *Can. J. Earth Sci.,* **22,** 1286–1298.

Kristoffersen, Y., 1978. Sea-floor spreading and the early opening of the North Atlantic, *Earth planet. Sci. Lett.,* **38,** 273–290.

Lau, K.H., Louden, K.E., Funck, T., Tucholke, B.E., Holbrook, W.S., Hopper, J.R. & Larsen, H.C., 2006a. Crustal structure across the Grand Banks-Newfoundland Basin continental margin - I. Results from a seismic refraction profile, *Geophys. J. Int.,* **167,** 127–156.

Lau, K.H., Louden, K.E., Deemer, S., Hall, J., Hopper, J.R., Tucholke, B.E., Holbrook, W.S. & Larsen, H.C., 2006b. Crustal structure across the Grand Banks-Newfoundland Basin continental margin - II. Results from a seismic reflection profile, *Geophys. J. Int.,* **167,** 157–170.

Le Pichon, X., Sibuet, J.-C. & Francheteau, J., 1977. The fit of continent around the North Atlantic Ocean, *Tectonophysics,* **38,** 169–209.

Li, Y. & Oldenburg, D.W., 1996. 3-D inversion of magnetic data, *Geophysics,* **61**(2), 394–408.

Li, Y. & Oldenburg, D.W., 1998. 3-D inversion of gravity data, *Geophysics,* **63,** 109–119.

Louden, K.E. & Chian, D., 1999. The deep structure of non-volcanic rifted continental margins, *Phil. trans. R. Soc. Lond.,* **357,** 767–804.

Makris, J., Egloff, R., Jacob, A.B., Mohr, P., Murphy, T. & Ryan, P., 1988. Continental crust under the southern Porcupine Seabight, West of Ireland, *Earth planet. Sci. Lett.,* **89,** 387–397.

Malinverno, A., 1991. Inverse square-root dependence of mid-ocean flank roughness on spreading rate, *Nature,* **352,** 58–60.

Murillas, J., Mougenot, D., Boillot, G., Comas, M., Banda, E. & Mauffret, A., 1990. Structure and evolution of the Galicia Interior Basin (Atlantic western Iberian continental margin), *Tectonophysics,* **184**(3–4), 297–319.

Naylor, D. & Shannon, P., 2009. Geology of offshore Ireland, in *The Geology of Ireland,* chapter 17, pp. 405–460, eds Holland, C.H. & Sanders, I.S., Dunedin Academic Press, Edinburgh, 2nd edn.

Peddy, C. & Hobbs, R., 1987. Lower crustal reflectivity of the continental margin southwest of Britain, *Ann. Geophys.,* **5B**(4), 331–338.

Peddy, C., Pinet, B., Masson, D., Scrutton, R., Sibuet, J.-C., Warner, M., Lefort, J., Shroeder, I., BIRPS & ECORS, 1989. Crustal structure of the Goban Spur continental margin, Northeast Atlantic, from deep seismic reflection profiling, *J. Geol. Soc. Lond.,* **146,** 427–437.

Pérez-Gussinyé, M. & Reston, T., 2001. Rheological evolution during extension at nonvolcanic rifted margins: onset of serpentinization and development of detachments leading to continental breakup, *J. geophys. Res.,* **106**(B3), 3961–3975.

Pérez-Gussinyé, M., Ranero, C., Reston, T. & Sawyer, D., 2003. Mechanisms of extension at nonvolcanic margins: evidence from the Galicia interior basin, west of Iberia, *J. geophys. Res.,* **108**(B5), doi:10.1029/2001JB000901.

Pickup, S., Whitmarsh, R., Fowler, C. & Reston, T., 1996. Insight into the nature of the ocean-continent transition off West Iberia from a deep multichannel seismic reflection profile, *Geology,* **24,** 1079–1082.

Reid, I., 1994. Crustal structure of a nonvolcanic rifted margin east of Newfoundland, *J. geophys. Res.,* **99**(B8), 15 161–15 180.

Reid, I. & Keen, C.E., 1990. High seismic velocities associated with reflections from within the lower oceanic crust near the continental margin of eastern Canada, *Earth planet. Sci. Lett.,* **99,** 118–126.

Reston, T., 2007. Extension discrepancy of North Atlantic nonvolcanic rifted margin: depth-dependent stretching or unrecognized faulting? *Geology,* **35**(4), 367–370.

Reston, T., Gaw, V., Pennell, J., Klaeschen, D., Stubenrauch, A. & Walker, I., 2004. Extreme crustal thinning in the south Porcupine Basin and the nature of the Porcupine Median High: implications for the formation of non-volcanic rifted margins, *J. Geol. Soc. Lond.,* **161**(5), 783–798.

Russell, S. & Whitmarsh, R., 2003. Magmatism at the west Iberia nonvolcanic rifted continental margin: evidence from analyses of magnetic anomalies, *Geophys. J. Int.,* **154**(3), 706–730.

Schreurs, G. & Colletta, B., 1998. Analogue modelling of faulting in zones of continental transpression and transtension, *Geol. Soc. Spec. Publ.,* **135,** 59–59.

Schroeder, T., John, B. & Frost, B., 2002. Geologic implications of seawater circulation through peridotite exposed at slow-spreading mid-ocean ridges, *Geology,* **30**(4), 367–370.

Shillington, D.J. *et al.*, 2006. Evidence for asymmetric nonvolcanic rifting and slow incipient oceanic accretion from seismic refraction data on the Newfoundland margin, *J. geophys. Res.,* **111**(B09402), doi:10.1029/2005JB003981.

Sibuet, J.-C., Srivastava, S. & Spakman, W., 2004. Pyrenean orogeny and plate kinematics, *J. geophys. Res.,* **109**(B08104), doi:10.1029/2003JB002514.

Sibuet, J.-C., Srivastava, S. & Manatschal, G., 2007a. Exhumed mantle-forming transitional crust in the Newfoundland-Iberia rift and associated magnetic anomalies, *J. geophys. Res.,* **112**(B06105), doi:10.1029/2005JB003856.

Sibuet, J.-C., Srivastava, S., Enachescu, M.E. & Karner, G., 2007b. Early Cretaceous motion of Flemish Cap with respect to North America: implications on the formation of Orphan Basin and SE Flemish Cap-Galicia Bank conjugate margins, in *Imaging, Mapping and Modelling Continental Lithosphere Extension and Breakup,* Geol. Soc. London, Special Publications,Vol. 282, pp. 63–76, eds Karner, G., Manatschal, G. & Pinheiro, L., Geological Society of London, London.

Srivastava, S. & Keen, C., 1995. A deep seismic reflection profile across the extinct Mid-Labrador Sea spreading center, *Tectonics,* **14,** 372–389.

Srivastava, S. & Roest, W., 1999. Extent of oceanic crust in the Labrador Sea, *Mar. Pet. Geol.,* **16**(1), 65–84.

Srivastava, S. & Sibuet, J.-C., 1992. A joint AGC and IFREMER geophysical cruise to the Newfoundland and Orphan Basins, Cruise Report CSS Hudson 92-22 Mission Erable (Unpublished Report), 121 pp., Geological Survey of Canada, Dartmouth, N.S. and Institut Français de Recherche pour l'Exploitation de la Mer, Centre de Brest.

Srivastava, S. & Verhoef, J., 1992. Evolution of Mesozoic sedimentary basins around the North Central Atlantic: a preliminary plate kinematic solution, in *Basins on the Atlantic Seaboard: Petroleum Geology, Sedimentology and Basin Evolution,*Vol. 62, pp. 397–420, ed. Parnell, J., Geological Society of London, London.

Srivastava, S., Verhoef, J. & Macnab, R., 1988a. Results from a detailed aeromagnetic survey across the northeast Newfoundland margin, Part I: spreading anomalies and the ocean-continent boundary, *Mar. Pet. Geol.,* **5,** 306–323.

Srivastava, S., Verhoef, J. & Macnab, R., 1988b. Results from a detailed aeromagnetic survey across the northeast Newfoundland margin, Part II: early opening of the North Atlantic between the British Isles and Newfoundland, *Mar. Pet. Geol.,* **5,** 324–336.

Srivastava, S., Roest, W., Kovacs, L., Oakey, G., Lévesque, S., Verhoef, J. & Macnab, R., 1990. Motion of Iberia since the Late Jurassic: results from detailed aeromagnetic measurements in the Newfoundland Basin, *Tectonophysics,* **184**(3–4), 229–260.

Srivastava, S., Sibuet, J.-C., Cande, S., Roest, W. & Reid, I., 2000. Magnetic evidence for slow seafloor spreading during the formation of the Newfoundland and Iberian margins, *Earth planet. Sci. Lett.,* **182**(1), 61–76.

Sullivan, K., 1983. The Newfoundland Basin: ocean-continent boundary and Mesozoic seafloor spreading, *Earth planet. Sci. Lett.,* **62**(3), 321–339.

Tucholke, B. & Sibuet, J.-C., 2007. Leg 210 synthesis: tectonic, magmatic and sedimentary evolution of the Newfoundland-Iberia rift, *Proc. Ocean Drill. Proj. Sci. Results,* **210,** 1–56.

Tucholke, B., Austin, J. & Uchupi, E., 1989. Crustal structure and rift-drift evolution of the Newfoundland basin, in *Extensional Tectonics and Stratigraphy of the North Atlantic Margins,*Vol. 46, chapter 16, pp. 247–263, eds Tankard, A. & Balkwill, H., AAPG Memoir, Tulsa, OK.

van Avendonk, H.J., Holbrook, W.S., Nunes, G.T., Shillington, D.J., Tucholke, B.E., Louden, K.E., Larsen, H.C. & Hopper, J.R., 2006. Seismic velocity structure of the rifted margin of eastern Grand Banks of Newfoundland, Canada, *J. geophys. Res.,* **111**(B11404), doi:10.1029/2005JB004156.

Welford, J., Smith, J., Hall, J., Deemer, S., Srivastava, S. & Sibuet, J.-C., 2010a. Structure and rifting evolution of the northern Newfoundland Basin from Erable multichannel seismic reflection profiles across the southeastern margin of Flemish Cap, *Geophys. J. Int.,* **180**(3), 976–998.

Welford, J., Shannon, P., O'Reilly, B. & Hall, J., 2010b. Lithospheric density variations and Moho structure of the Irish Atlantic continental margin from constrained 3-D gravity inversion, *Geophys. J. Int.,* **183**, 79–95, doi:10.1111/j.1365-246X.2010.04375.x.

White, R., 1992. Crustal structure and magmatism of North Atlantic continental margins, *J. geol. Soc. Lond.,* **149,** 841–854.

Whitmarsh, R. & Wallace, P., 2001. The rift-to-drift development of the west Iberia nonvolcanic continental margin: a summary and review of the contribution of ocean drilling program leg 173, *Proc. Ocean Drill. Proj. Sci. Results,* **173,** 1–36.

Whitmarsh, R., White, R.S., Horsefield, S.J., Sibuet, J.-C., Recq, M. & Louvel, V., 1996. The ocean-continent boundary off the western continental margin of Iberia: crustal structure west of Galicia Bank, *J. geophys. Res.,* **101**(B12), 28291–28314.

Whitmarsh, R., Manatschal, G. & Minshull, T., 2001a. Evolution of magma-poor continental margins from rifting to seafloor spreading, *Nature,* **413**(6852), 150–154.

Williams, C., 1975. Sea-floor spreading in the Bay of Biscay and its relationship to the North Atlantic, *Earth planet. Sci. Lett.,* **24**(3), 440–456.

Williams, H., 1984. Miogeoclines and suspect terranes of the Caledonian-Appalachian orogen: tectonic patterns in the North Atlantic region, *Can. J. Earth Sci.,* **21,** 887–901.

Williams, H., 1995. *Geology of the Appalachian-Caledonian* orogen in Canada and Greenland, Geological Survey of Canada, Geology of Canada, no. 6.

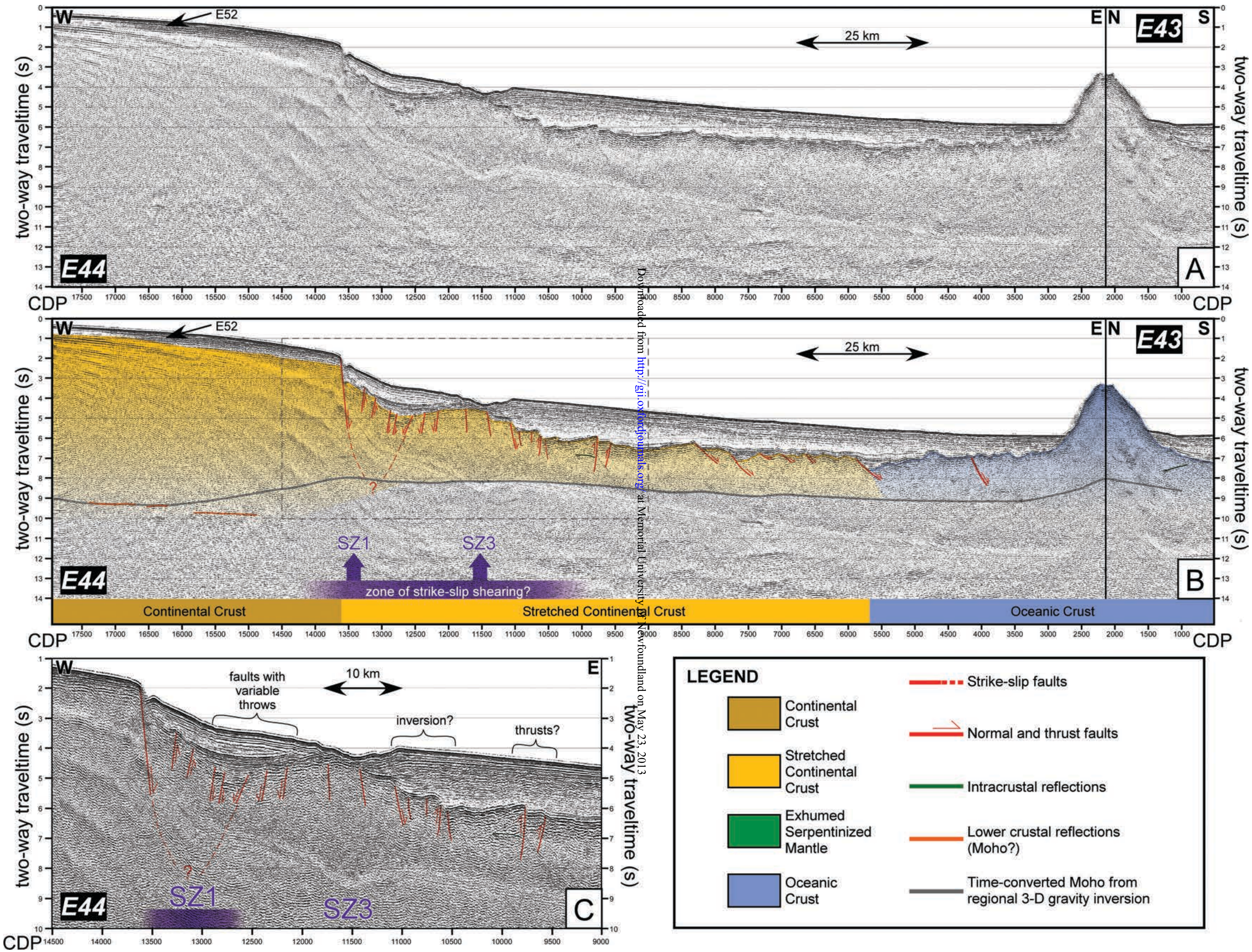

Figure 3. (A) Time migration of the Erable 43 and 44 (E43 and E44) seismic reflection profiles with the corresponding interpretation of crustal domains (B). An enlarged portion of the data outlined by the dashed grey box in (B) is shown in (C) underlain by the fault interpretations and with slightly different plotting parameters. The legend below the figure explains the shading and line colours used in the interpretation. Crossovers with other seismic lines are identified with black arrows. The purple arrows and shading in (B) and (C) highlight interpreted SZs. The interpretations of crustal boundaries, labelled along the bottom of plot B, are discussed in the text.

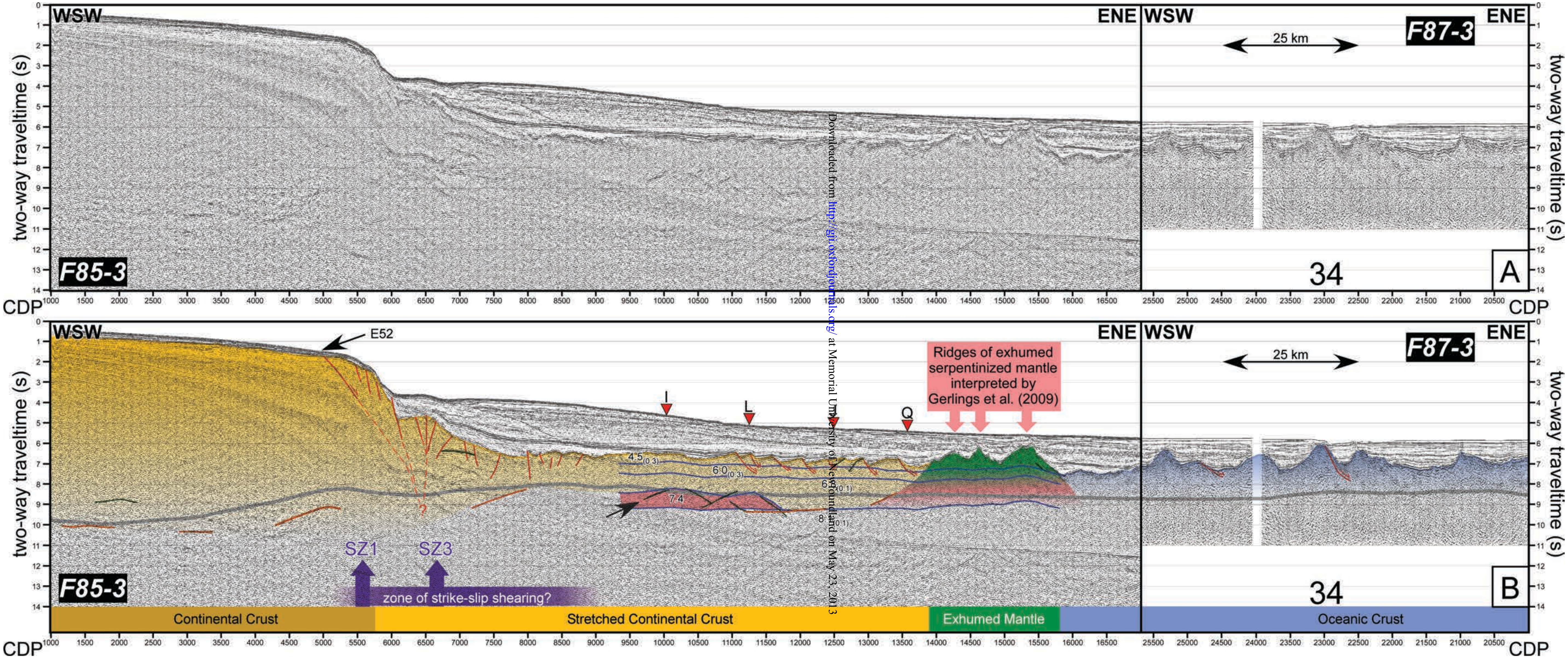

Figure 4. (A) Time migration of the combined F85-3 and F87-3 seismic reflection profiles from the FGP project (Keen *et al*. 1987; Reid & Keen 1990) with the corresponding interpretation of crustal domains (B). The location of magnetic anomaly 34 by Srivastava *et al*. (1988b) is shown at the bottom of the sections. The grey arrow in (B) highlights the landward-dipping reflector interpreted as the continent–ocean boundary by Keen & de Voogd (1988). The inverted red triangles labelled with letters along the seabed in B correspond to the OBS used in the seismic refraction survey of Reid & Keen (1990). The velocity model crustal boundaries from that study are underlain as blue lines between CDPs 9400 and 16000 with the topmost velocities and the gradients (in parentheses) within those layers annotated. The pink shading highlights an anomalous zone with a velocity of 7.4 km s^{-1} modelled from the refraction data (Reid & Keen 1990). Refer to the legend in Fig. 3 for explanation of all other shading and line colours in B. Remaining caption as in Fig. 3.

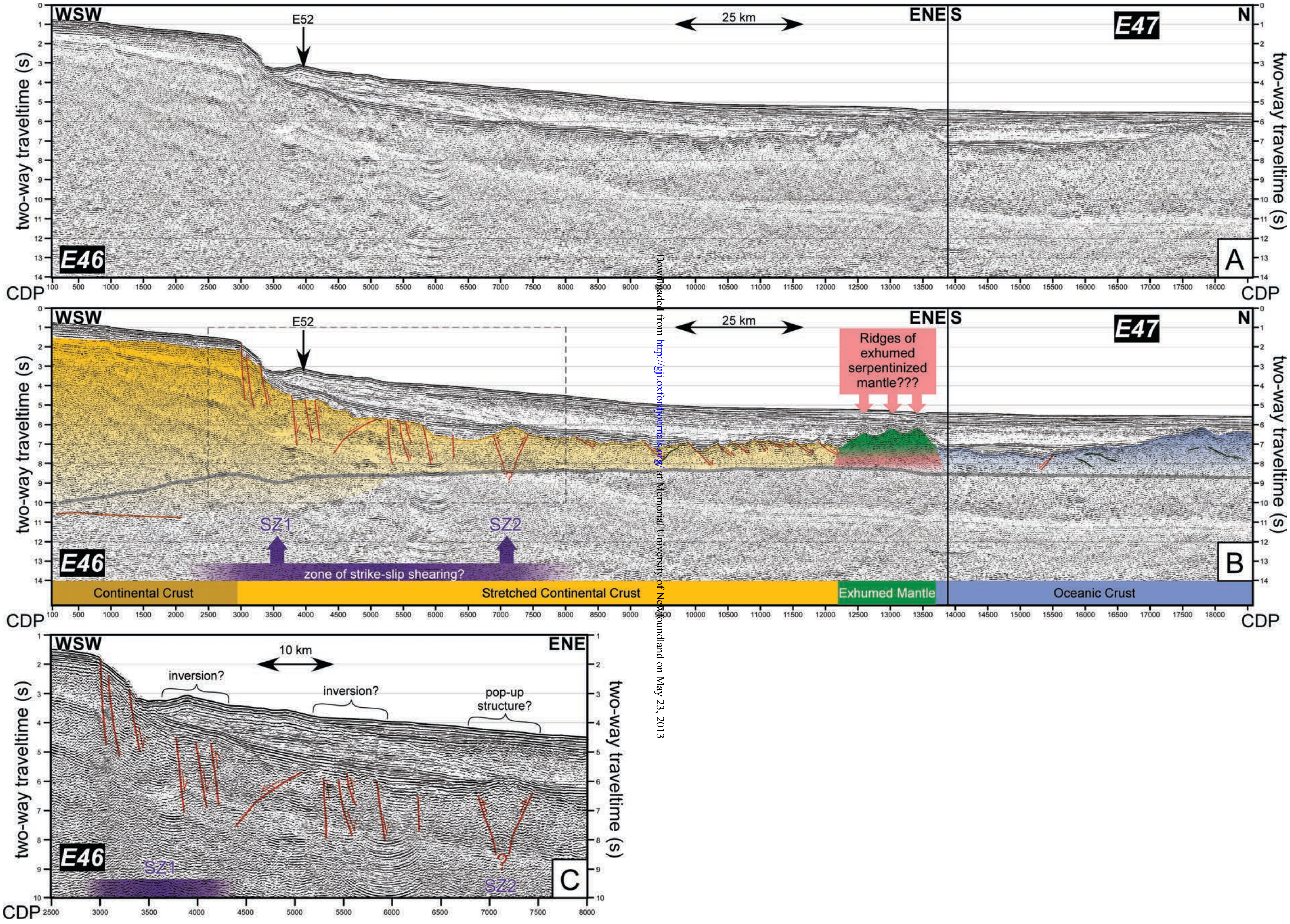

Figure 5. (A) Time migration of the Erable 46 and 47 (E46 and E47) seismic reflection profiles with the corresponding interpretation of crustal domains (B) and an enlarged data section (C). Refer to the legend in Fig. 3 for explanation of shading and line colours in B. Remaining caption as in Fig. 3.

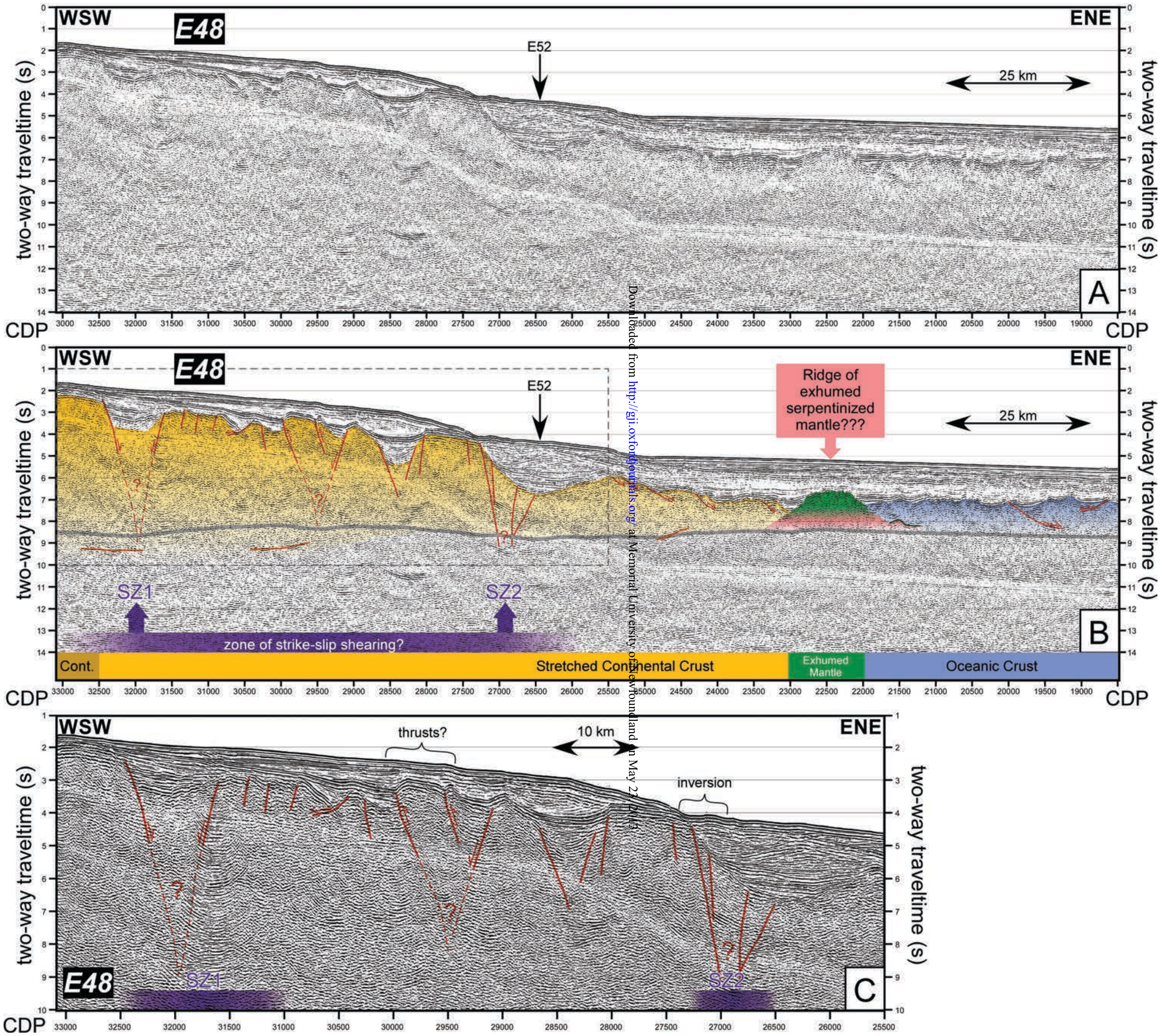

Figure 6. (A) Time migration of the Erable 48 (E48) seismic reflection profile with the corresponding interpretation of crustal domains (B) and an enlarged data section (C). Refer to the legend in Fig. 3 for explanation of shading and line colours in B. Remaining caption as in Fig. 3.

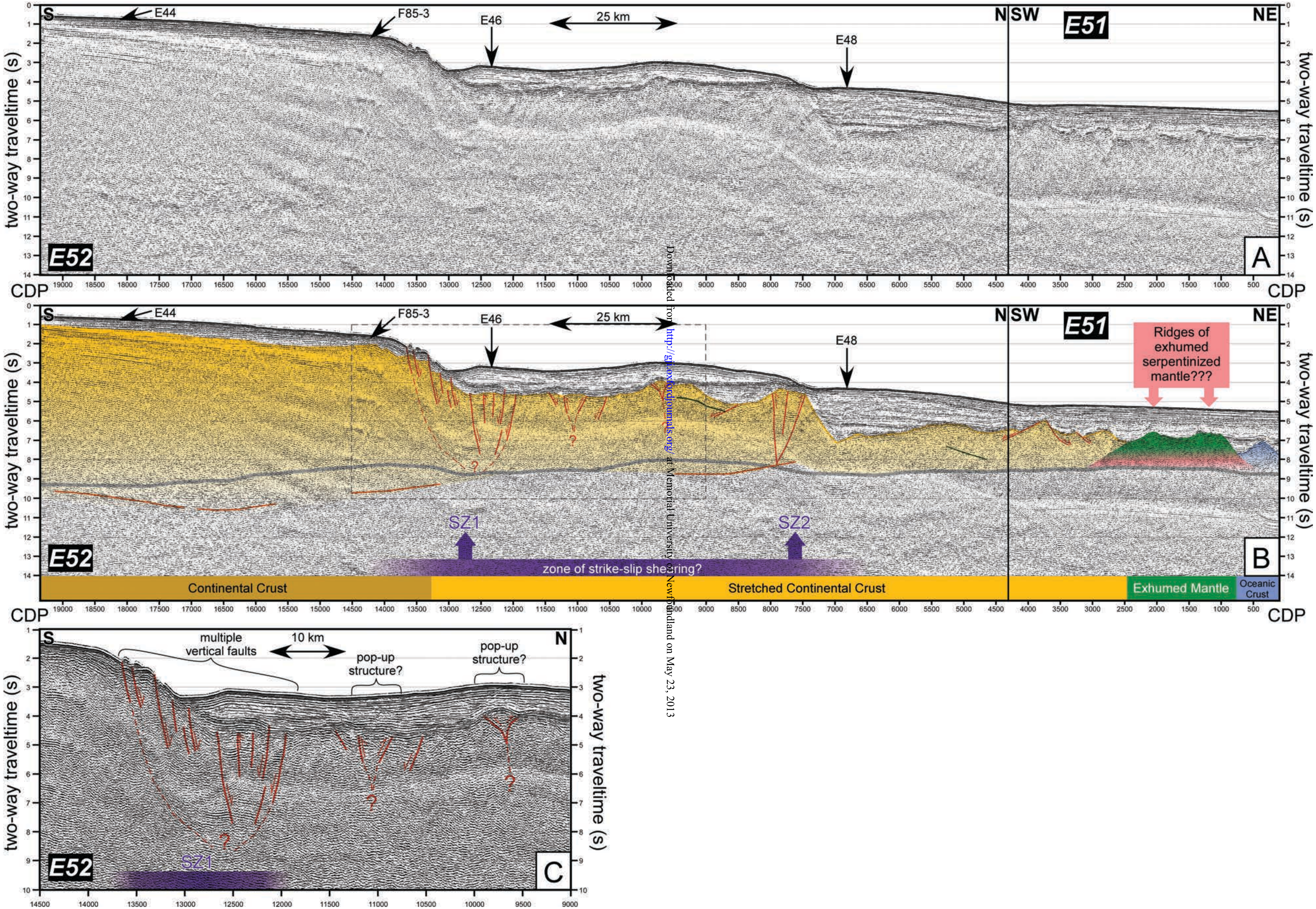

Figure 7. (A) Time migration of the Erable 51 and 52 (E51 and E52) seismic reflection profiles with the corresponding interpretation of crustal domains (B) and an enlarged data section (C). Refer to the legend in Fig. 3 for explanation of shading and line colours in B. Remaining caption as in Fig. 3.

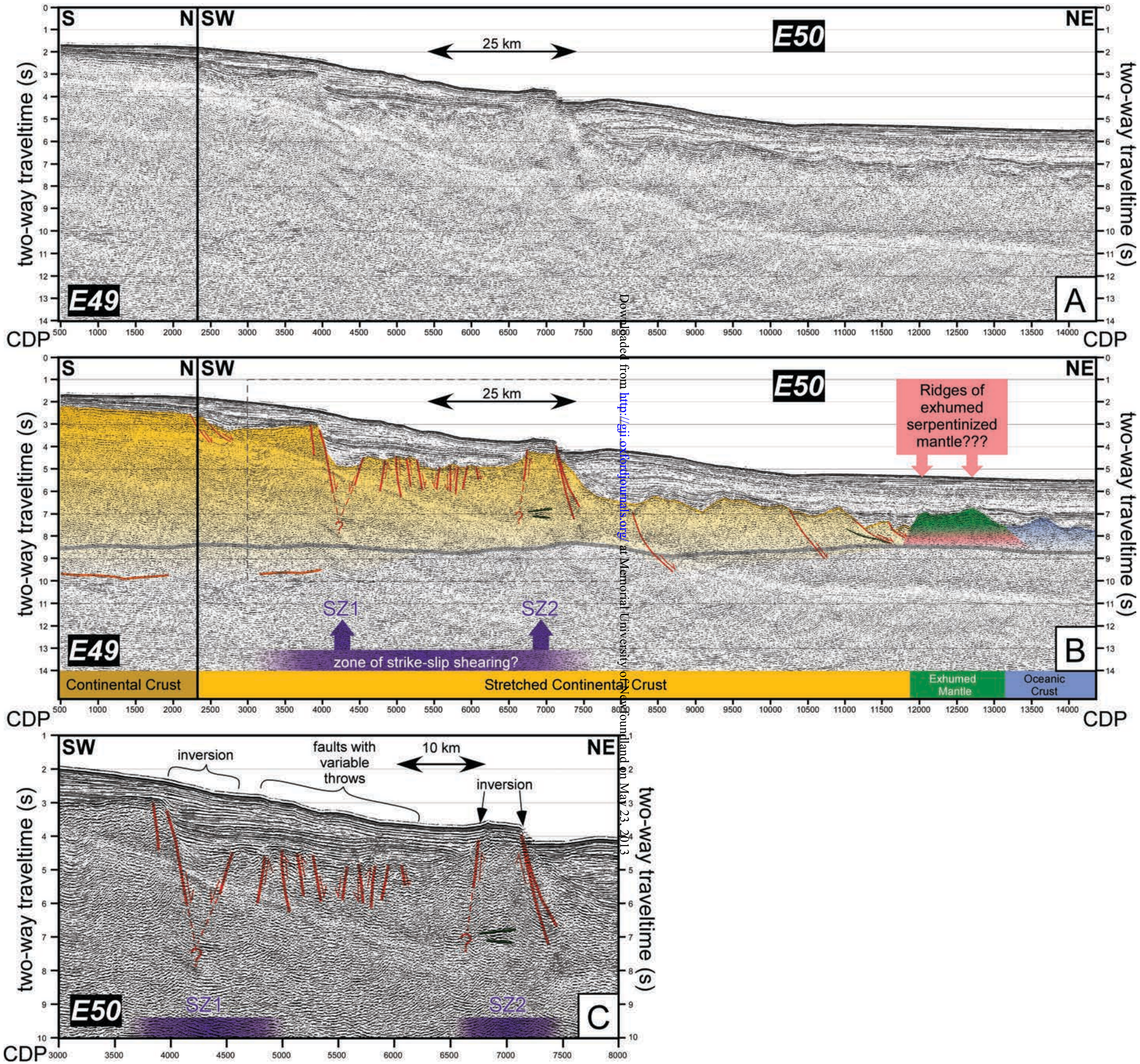

Figure 8. (A) Time migration of the Erable 49 and 50 (E49 and E50) seismic reflection profiles with the corresponding interpretation of crustal domains (B) and an enlarged data section (C). Refer to the legend in Fig. 3 for explanation of shading and line colours in B. Remaining caption as in Fig. 3.

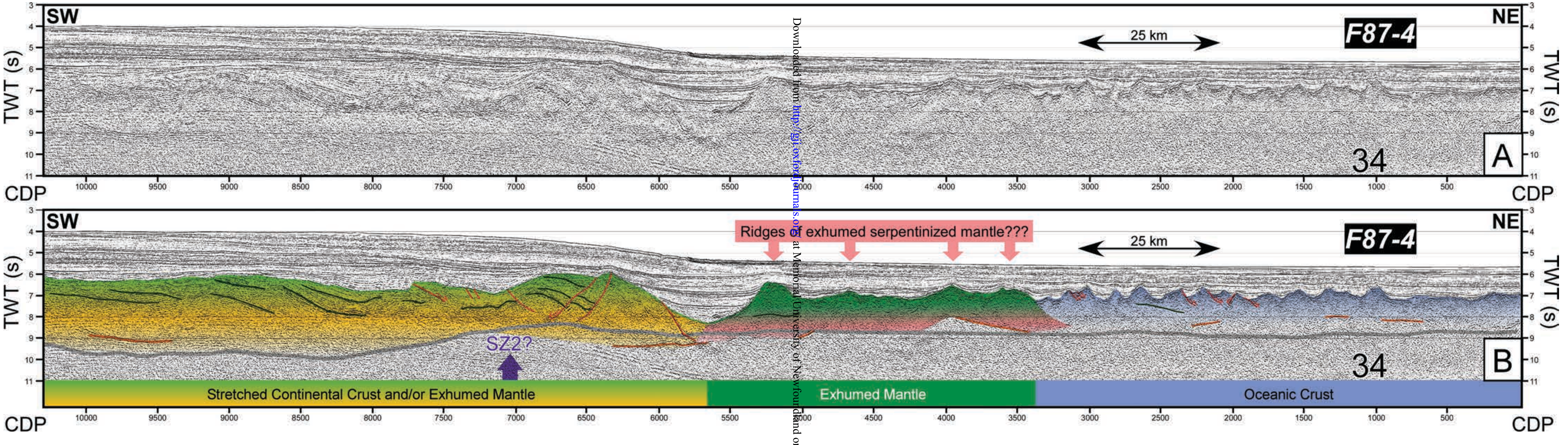

Figure 9. (A) Time migration of the F87-4 seismic reflection profile from the FGP project with the corresponding interpretation of crustal domains (B). Refer to the legend in Fig. 3 for explanation of shading and line colours in B. The location of magnetic anomaly 34 by Srivastava *et al*. (1988b) is shown at the bottom of the sections.